



Historical perspective

Biomimetic multifunctional surfaces inspired from animals

Zhiwu Han, Zhengzhi Mu, Wei Yin, Wen Li, Shichao Niu *, Junqiu Zhang *, Luquan Ren

Key Laboratory of Bionic Engineering (Ministry of Education, China), Jilin University, Changchun 130022, P.R. China



ARTICLE INFO

Available online 31 March 2016

Keywords:

Biomimetic
Multifunctional surface
Surface function
Surface structure
Surface morphology

ABSTRACT

Over millions of years, animals have evolved to a higher intelligent level for their environment. A large number of diverse surface structures on their bodies have been formed to adapt to the extremely harsh environment. Just like the structural diversity existed in plants, the same also applies true in animals. Firstly, this article provides an overview and discussion of the most common functional surface structures inspired from animals, such as drag reduction, noise reduction, anti-adhesion, anti-wear, anti-erosion, anti-fog, water capture, and optical surfaces. Then, some typical characteristics of morphologies, structures, and materials of the animal multifunctional surfaces were discussed. The adaptation of these surfaces to environmental conditions was also analyzed. It mainly focuses on the relationship between their surface functions and their surface structural characteristics. Afterwards, the multifunctional mechanisms or principles of these surfaces were discussed. Models of these structures were provided for the development of structure materials and machinery surfaces. At last, fabrication techniques and existing or potential technical applications inspired from biomimetic multifunctional surfaces in animals were also discussed. The application prospects of the biomimetic functional surfaces are very broad, such as civil field of self-cleaning textile fabrics and non-stick pots, ocean field of oil–water separation, sports field of swimming suits, space development field of lens arrays.

© 2016 Elsevier B.V. All rights reserved.

Contents

1. Introduction	28
2. Natural multifunctional surfaces in animals and their characteristics	29
2.1. Surfaces for anti-wear	29
2.2. Surfaces for superhydrophobicity	29
2.3. Surfaces acting as smart adhesives	30
2.4. Surfaces for drag reduction	30
2.5. Optically functional surface	30
2.6. Surfaces for anti-fogging	31
2.7. Surfaces for noise reduction	31
2.8. Surfaces for water capture	31
3. Modeling and design	34
3.1. Modeling of self-cleaning for gecko setae	34
3.2. Modeling of superhydrophobic	34
3.2.1. Modeling of superhydrophobic for water striders	34
3.2.2. Modeling of superhydrophobic for gecko feet	34
3.2.3. Modeling of directional adhesion of superhydrophobic for butterfly wings	35
3.3. Modeling of superoleophobicity for fish scales	35
3.4. Modeling of frictional adhesion	36
3.5. Modeling of light trapping	37
3.6. Modeling of fluid-drag reduction	37
3.7. Modeling of erosion resistance	37
4. Fabrication approaches	38
4.1. Chemical routes	38
4.1.1. Sol-gel	38

* Tel.: +86043185095760-615.

E-mail addresses: niushichao@jlu.edu.cn (S. Niu), zhangjunqiu2005@163.com (J. Zhang).

4.1.2.	Etching	40
4.1.3.	Sonochemical	40
4.1.4.	Chemical vapor deposition (CVD) and chemical vapor infiltration (CVI)	41
4.1.5.	Atomic layer deposition (ALD)	41
4.1.6.	Assembly methods	41
4.2.	Physical routes	42
4.2.1.	Physical evaporation and deposition	42
4.2.2.	Imprinting	42
4.2.3.	Direct laser writing	43
4.3.	Template removal	43
4.3.1.	Calcination	44
4.3.2.	Selective dissolution	44
4.3.3.	Sonication	44
5.	Applications	44
5.1.	Self-cleaning super-amphiphobic	44
5.2.	Biomimetic adhesion	45
5.3.	Biomimetic non-adhesive	45
5.4.	Engineering drag-reduction	46
6.	Summary	47
	Acknowledgements	48
	References	48

1. Introduction

Biologically inspired design, adaptation, or derivation from nature is referred to as "**biomimetics**". It means mimicking biology or nature. The field of biomimetics is highly interdisciplinary. It involves the understanding of biological functions, structures, and principles of various objects found in nature. The word "biomimetics" firstly appeared in Webster's dictionary in 1974 and is defined as the study of the formation, structure or function of biologically produced substances and materials (as enzymes or silk) and biological mechanisms and processes (as protein synthesis or photosynthesis) especially for the purpose of synthesizing similar products by artificial mechanisms which mimic natural ones [1].

After billions of years of evolution, creatures in nature possess almost perfect structures and functions [2]. Animals, like humans, are always striving for a better survival on earth. They come up with widely different and highly creative survival strategies through long-time evolution. Focusing on animal multi-functional surfaces, an animal itself is an intricate system as a result of long-time evolution. Animals have developed amazing functions in order to avoid predator, prey, mate choice and adapt to their harsh living environments, etc.

Firstly, protective resemblance is always used to avoid predation. It includes special protective resemblance, now called mimesis, where the whole animal looks like some another object. For example, a caterpillar always resembles a twig or a bird dropping. In general protective resemblance, now called crypsis, the animal's texture blends with the background. For example, a moth's color and pattern blend in with tree bark. Butterflies are universally attractive because of their bright iridescences. These colorations serve many purposes in insect groups, including camouflage, which is utilized to elude from their predators; warning role, utilized as mimic of bad-tasting butterflies [3].

Secondly, in order to prey, some animals must evolve some excellent functional structures that are restraint or superior to their preys. On the one hand, some animals become silent during their flights, for example, the owl's silent flight. Many species of owls have the ability to fly silently. The quiet owl in both gliding and flapping flight generates noise at low frequencies below 2 kHz, which is below its prey's hearing range (2 kHz to 20 kHz) [4]. Some animals become much faster and more sensitive during their movement towards their preys, for example, the water striders. Jiang et al. found that a leg of the water striders can support a weight equivalent to 15 times of their own body weight and would not sink. The speed of its gliding per second could be 100 times of its body distance, which is equivalent to one person with a height

of 1.8 m swim at a speed of 400 miles per hour. All of that ensure that the water striders could glide on the surface of the water fast and be flexible at an extremely high speed to prey its prey [5].

Thirdly, a growing number of studies suggest that iridescence plays an important role in mate choice. In the butterfly *Eurema hecabe*, males with intact ultraviolet (UV) reflectance experience greater copulation success than males with experimentally reduced UV reflectance, and in naturally occurring copulations, males with more UV reflectance copulated with larger females [6]. Similar preferences for UV iridescence were documented in the butterflies *Hypolimnas bolina* [7], *Heliconius cydno* [8] and *Colias eurytheme* [9]. Despite compelling evidence that iridescent coloration appears to be an important mate choice cue in some species, a few studies have also failed to detect an influence of iridescence on mate choice [10]. Butterflies are universally attractive because of their bright iridescences. These colorations serve many purposes in insect groups, including camouflage, which is utilized to elude from their predators; warning role, utilized as mimic of bad-tasting butterflies; mate choice, utilized to find and attract their mates [3].

Properties of animals' functional surfaces result from a complex interplay between surface morphologies and physical and chemical properties. Hierarchical structures with dimensions of features ranging from the macroscale to the nanoscale are extremely common in nature to provide properties of interest. Animals have learned how to achieve most efficient multi-functional surfaces. The optimized biological solution should give us inspirations and design principles for the construction of multi-functional artificial surfaces. In the last few decades, inspired by the typical animal functional surfaces, a great number of multi-functional surfaces have been fabricated. This article has focused on the typical animals' surfaces with drag reduction, noise reduction, anti-adhesion, anti-wear, anti-erosion, anti-stealthy, anti-fog, low reflection of light, and others. The development of animal functional surfaces is important for basic research as well as various applications, including super-amphiphobic textiles, self-cleaning nano-tie, stickybot and applications requiring anti-fouling and a reduction in fluid flow.

In general, learning from nature has long been a source of bio-inspiration for scientists, engineers, human kind [11–17]. In recent decades, a great number of animals' functional surfaces have been investigated by scientists and engineers from various fields. Progress in some typical animals' functional surfaces, such as drag reduction, noise reduction, surfaces that act as smart adhesives, anti-wear, anti-erosion, anti-fog, optically functional surfaces, and others, was discussed. This review contains six sections. Section 1 is Introduction. Section 2 presents the natural multifunctional surfaces in animals and their characters.

Section 3 is principle of evolution. **Section 4** is modeling and design. **Section 5** is processing. **Section 6** is applications. Finally, we discuss challenges and perspectives for animals' functional surface in the future. This paper does not have the aim to present a complete review but to discuss some new and important results.

2. Natural multifunctional surfaces in animals and their characteristics

Firstly, the multifunction of the animals' surfaces should be introduced, including anti-wear functional surfaces, superhydrophobic functional surfaces, surfaces that act as smart adhesives, drag reduction functional surfaces, optically functional surfaces, anti-fog functional surfaces, noise reduction functional surfaces and water capture functional surfaces. In this part, the characteristics of these surfaces were introduced, such as the typical biology, the key parts of animals' bodies and surface morphology features of their bodies.

2.1. Surfaces for anti-wear

For the biology survived in desert, wear and tear of the sand wind on their body surface are the first big challenge. On the other hand, wear is also undesirable and can lead to catastrophic failure in most industrial applications [18]. It limits the lifetime of components and therefore when parts fail the problem of their recycling also arises. Fortunately, there exist numerous cases of soil-burrowing animals having peculiar surface geometries specifically evolved to resist against soil wear and prevent soil to adhere to the animals' bodies. Animals that have recently been investigated include the dung beetle (*Copris ochus Motschulsky*), the ground beetle (*Carabidae*), the earthworm (*Lumbricidae*), the *Oniscidae*, the *Diplopoden*, the centipede (*Chilopoda*), the ant (*Formicidae*), and the mole cricket (*Gryllotalpidae*) [19] (Fig. 1).

In addition, marine biological systems, such as seashells and whelks, also have corrugated shells optimized to survive in highly abrasive slurry environments [20]. Tian et al. [21] studied the anti-wear properties of three typical shells. According to their analysis, the non-equal-lattice geometric network morphology of *S. Subcrenata* has an excellent property of wear resistance. Tong et al. [22,23] showed that abrasive wear features of different mollusk shells, including *Lamprotula fibrosa Heude* (a kind of mussel), *Rapana venosa Valenciennes* (veined rapa whelk) and *Dosinia anus Philippi* (old-woman dosinia), have directionality. The analysis showed that the abrasive wear of these three shells, mainly due to micro-shoveling and micro-cracking, increases with the size and sliding velocity of the abrasive particle.

Erosion is one of the wear problems for material damage or equipment failure. It also causes millions of dollars of damage each year to helicopter rotors, rocket motor nozzles, turbine blades, pipes and other mechanical parts [25,26]. In nature, some animals such as desert lizards and scorpions are living in the sand and other gas/solid mixed-media environment, which exhibit excellent anti-erosion function under gas/solid mixed media environment through synergistic action of special surface morphology, internal microstructure and biological flexibility. Scorpion back has the ability to resist erosion without damage (Fig. 2). Han and Zhang et al. [25–27] showed the erosion resistance mechanism of scorpion back, which is a result of multiple coupling effects. Surface morphology, material and flexibility are biological coupling elements which play an important role in resistance to erosion by the back of desert scorpion. According to their analysis, scorpions, through the adaptation to the living environment and their own evolution, can form a special distribution of the convex and groove on the back, which can change the state of the surface boundary layer flow, hence, reduce erosion of surface (Fig. 2(d)). On the other hand, intersegment membrane and lateral membrane with flexibility play the role of energy release, helping to reduce erosion.

2.2. Surfaces for superhydrophobicity

Superhydrophobic surfaces are characterized by static contact angles with water (θ_w) above 150° . The superhydrophobicity (hydrophobicity) of solid surfaces has been investigated with considerable attention over the past few years and remarkable progress has been achieved [28]. Recent research has indicated that there are many superhydrophobic surfaces in nature [29–32], and this helps to promote the applications of biomimetic ideas into practical fields [33–35].

In nature, some animal surfaces with hierarchical structure and roughness can produce significant superhydrophobicity. Strider have the ability to stand and walk upon a water surface without getting wet (Fig. 3). Gao and Jiang [5] showed that the special hierarchical structure of the strider's legs, which are covered by large numbers of oriented tiny hairs (microsetae) with fine nanogrooves and covered with cuticle wax, makes the leg surfaces superhydrophobic, is responsible for the water resistance, and enables them to stand and walk quickly on the water surface. On the other hand, the scales on the wing surfaces of some butterflies have regularly arranged edges which are overlapping like roof tiles [31,36], as shown in Fig. 4a-c. The lengths and widths of each individual scales are roughly ranged 50–150 μm and 35–70 μm , respectively, while the primary distance between the middle points on the long axis of two adjacent scales is within 100 μm . According to their analysis [31], the lower capacity of *Parnassius* butterfly wing

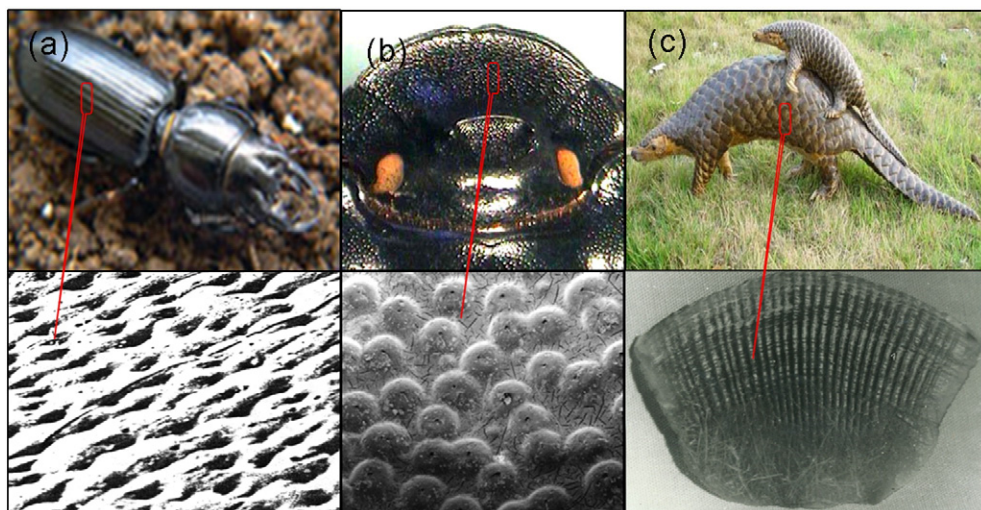


Fig. 1. Peculiar surface geometries of soil-burrowing animals. (a) Ground beetle; (b) Dung beetle; (c) Pangolin. Reproduced from reference [19,24] with permission from Elsevier.

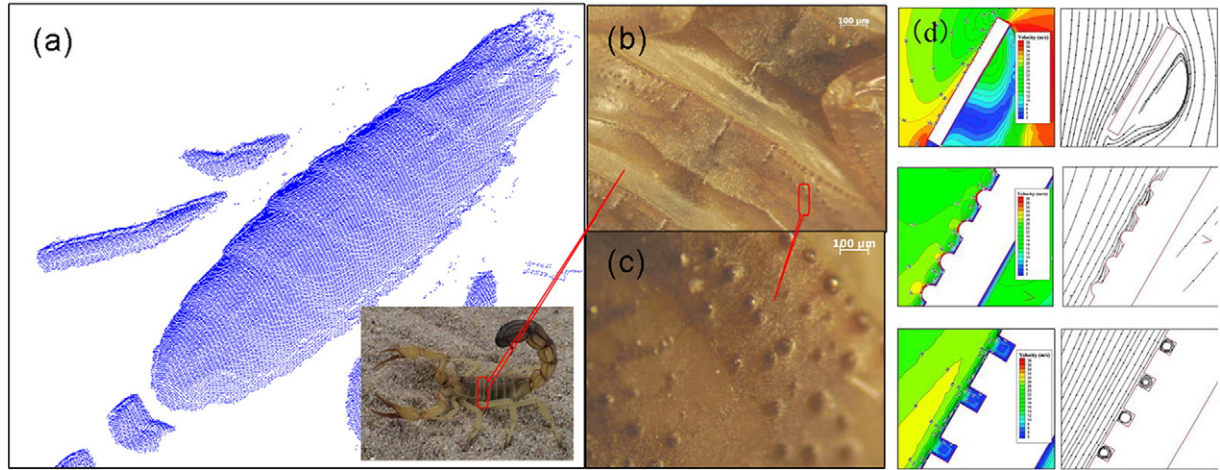


Fig. 2. The dorsal surface of the scorpion. (a) Scanned data using a laser scanner; (b) The convex hull of scorpion back; (c) The groove of scorpion back; (d) Mechanism of the anti-wear surface of scorpion: The air was rotating in the groove channel, forming a stable low-speed reverse flow zone. Adapted from reference [25] with permission from the American Chemical Society.

surfaces to resist methanol wetting is due to the special micro-structure of the scales (spindle-like shape) and ultra-structure (pinnule-like shape).

Phenomenologically, Byun et al. selected 10 orders and 24 species of insects to characterize the functions of natural structures by focusing on both lower and upper surfaces of the wings [32]. They argued that the hierarchical architectures which included micro- and nanoscale layers on the upper surfaces of insect wings (Fig. 5) promoted hydrophobicity, thereby enabling water droplets to roll off the wings and remove the dirt particles.

2.3. Surfaces acting as smart adhesives

A gecko is the largest animal that can produce high (dry) adhesion to support its weight with a high factor of safety [38]. The ability of gecko (Fig. 6a) running up and down a vertical surface was observed in ancient time, however, only with the advent of the electron microscopy in the 1950s, it became possible to view a complex hierarchical morphology that covers the skin on the gecko's foot (Fig. 6b) and toes (Fig. 6c). The skin comprises a complex fibrillar structure of lamellae, setae, branches, and spatula (Fig. 6d) [39–47]. This hierarchical structure allows a gecko to attach to and detach from the surfaces at will. An explanation of the gecko's ability to control adhesion is in its ability to adapt to the surface roughness and achieve very large real areas of contact between the gecko's foot and the surface [42,48]. The compliance and adaptability of setae are the primary sources of high adhesion.

On the other hand, the problem of soil adhesion has been solved by the soil-burrowing animals. They can move in soil without soil sticking to their bodies, especially in clay. Research shows that they have a

significant ability to prevent soil from sticking to their bodies because of the evolution of their biological systems through the exchange of matter, energy and information with soil over millions of years [24].

2.4. Surfaces for drag reduction

Underwater animals (such as carp, shark) can swim freely owing to their special surface structures. For carps, sector like scales are covered by oriented micropapillae with nanostructures (Fig. 7), presenting not only drag-reducing function but superoleophilicity in air and superoleophobicity in water [49,50]. The superoleophobic fish surface originates from the water-phase micro/nano hierarchical structures.

Shark skin, which is a model from nature for a low drag surface, is covered by very small individual tooth-like scales called dermal denticles (little skin teeth), ribbed with longitudinal grooves (aligned parallel to the local flow direction of the water). These grooved scales reduce the formation of vortices present on a smooth surface, resulting in water moving efficiently over their surface [52,53]. An example of scale structure on the right front of a Galapagos shark (*Carcharhinus galapagensis*) is shown in Fig. 8.

Also, birds have wings that consist of several consecutive rows of feathers, which are flexible. These movable flaps develop the lift. When a bird lands, a few feathers are deployed in front of the leading edges of the wings, which help to reduce the drag on the wings [31].

2.5. Optically functional surface

Microstructure surfaces for various optical applications include non-reflective surfaces, highly reflective surfaces, colored (in some cases,

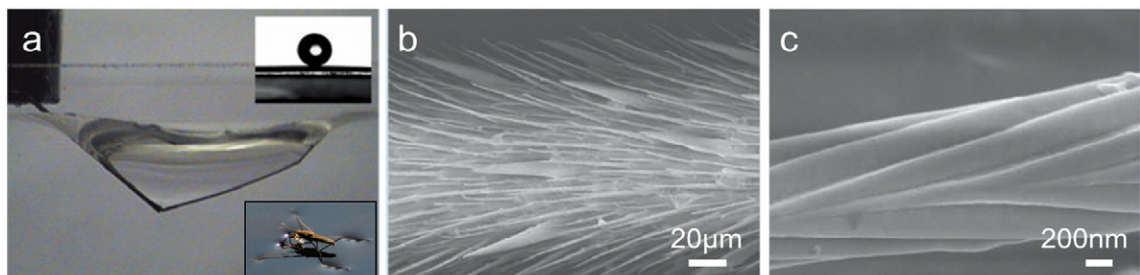


Fig. 3. Pond skater walking on water. Adapted from reference [5] with permission from Nature Publishing Group.

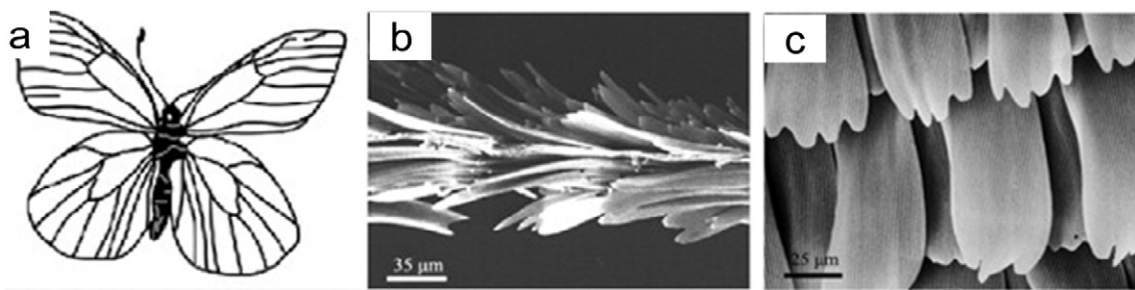


Fig. 4. Natural hierarchical surfaces. (a) Schematic of a butterfly (*Pontia daplidice*); (b) SEM image shows the transaction of the butterfly wing surface; (c) SEM image of its flat arranging of butterfly scales. Adapted from reference [37] with permission from Elsevier.

including the ability to dynamically control coloration) surfaces and transparent surfaces [18]. Han et al. [54] investigated the efficient light trapping effect of a typical butterfly *Trogonoptera brookiana* and found that the light trapping structures which cause the iridescent colors are composed by two distinct completely different types of nanostructures (one on the front and one on the back of the wing). The UV light and most visible light energy (other than the blue light) were trapped into the nanostructures on butterfly wing scales through the multilayer interference of the shelf structure and the diffraction gratings of the quasi-honeycomb-like structure. In addition, in order to avoid predators, the color of butterfly wings would be changed in the wake of the variation of the incident light angle, resulting in the color and brightness of the butterfly wings are consistent with background. Han et al. [55–57] found that a certain frequency of light would be absorbed or diffracted by the nano-structures on butterfly wings, achieving the stealth effect (Fig. 9) [54].

On the other hand, eyes of moths are antireflective to visible light and consist of hundreds of hexagonally organized nanoscopic pillars, each approximately 200 nm in diameter and height, which result in a very low reflectance for visible light [58]. These nanostructural optical surfaces make the eye surface nearly antireflective in any direction.

2.6. Surfaces for anti-fogging

Gao et al. [59] found that the compound eyes of the mosquito *C. pipiens* possess ideal superhydrophobic properties that provide an effective protective mechanism for maintaining clear vision in a humid habitat (Fig. 10). According to their analysis, this unique property is attributed to the smart design of elaborate micro- and nanostructures: hexagonally non-close-packed (NCP) nipples at the nanoscale prevent

microscale fog drops from condensing on the ommatidia surface, and hexagonally close-packed (HCP) ommatidia at the microscale could efficiently prevent fog drops from being trapped in the voids between the ommatidia.

2.7. Surfaces for noise reduction

Many species of owls are able to fly quietly (Fig. 11). The acoustic measurement and microscopic observation of the eagle owl (*Bubo bubo*) [4] show that the eagle owl generates lower sound intensity and lower frequency flight noise and the wing feather of the eagle owl has great sound absorption property. The microscopic structures of three special characteristics of feather are help to improve the pressure fluctuation of turbulence boundary, and suppress the generation of vortex noise.

2.8. Surfaces for water capture

In areas of limited water, for example, the Namib Desert, nature has developed elegant schemes for harvesting water from the atmosphere. The superhydrophobic patterns on the Namib Desert Stenocara beetle's back is a good example of the microcondensation of water [60]. The Stenocara beetle in the Namib Desert uses the hydrophilic/superhydrophobic patterned surface of its wings (shown as Fig. 12) to collect drinking water from fog-laden wind. This beetle's back is comprised of hydrophilic hills and superhydrophobic channels. The former can collect water from the fogs in the desert atmosphere and the latter can help the water droplet thus collected flow down to the beetle's mouth. After these small water droplets coalesce into bigger droplets, they roll down into the beetle's mouth, providing the beetle with a

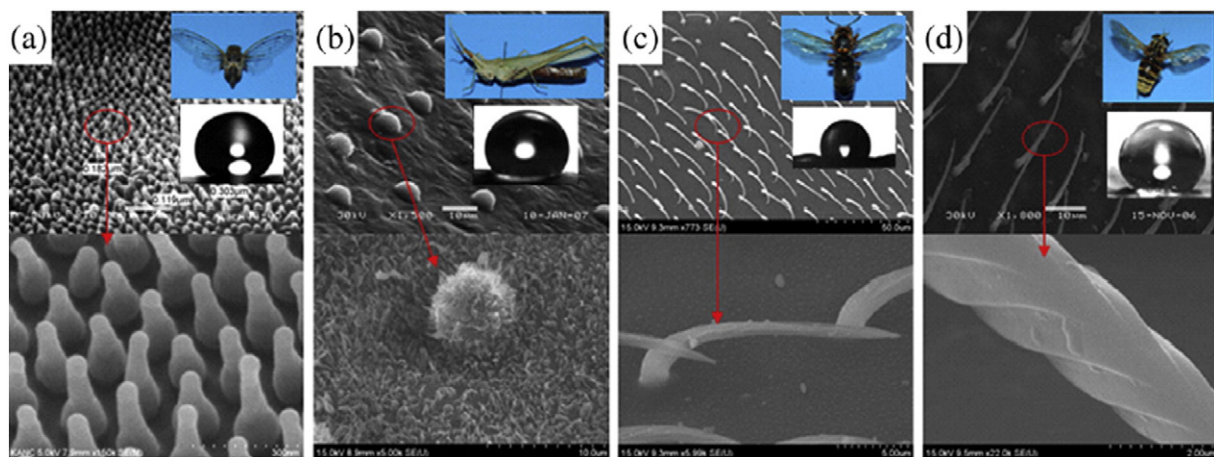


Fig. 5. SEM images of the micro/nano structures and measured contact angles on upper wing surfaces of insects. (a) Homoptera *Meimuna opalifera* (Walker); (b) Orthoptera *Acrida cinerea* (Thunberg); (c) Hymenoptera *Vespa dybowskii* (Andre); (d) Diptera *Tabanus chrysurus* (Loew). Adapted from reference [32] with permission from Elsevier.

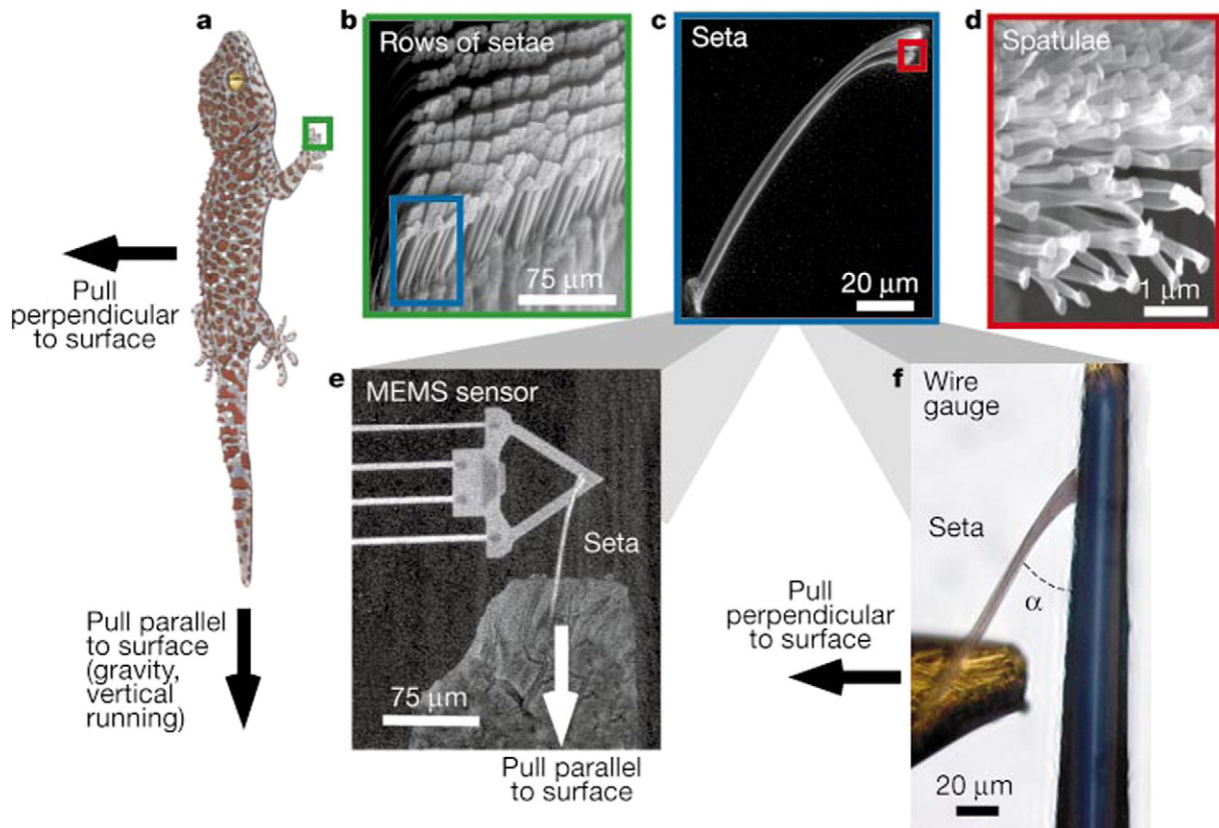


Fig. 6. Gecko setae and apparatus for force measurement. (a) Photo of the Tokay gecko (*Gekko gecko*); (b) SEM image of arrays of setae from a toe; (c) A single seta; (d) The finest terminal spatula of a seta; (e) Single seta attached to a micro-electromechanical system (MEMS) cantilever capable of measuring force production during attachment parallel and perpendicular to the surface; (f) Single seta attached to an aluminum bonding wire capable of measuring force production during detachment perpendicular to the surface. Reproduced from reference [46] with permission from Nature Publishing Group.

fresh morning drink [60,61]. Research shows that these large droplets form by virtue of the insect's bumpy surface, which consists of alternating hydrophobic, wax-coated and hydrophilic, non-waxy regions. The

design of this fog-collecting structure can be reproduced cheaply on a commercial scale and may find application in water-trapping tent and building coverings [60]. Inspired by this wonderful natural design,

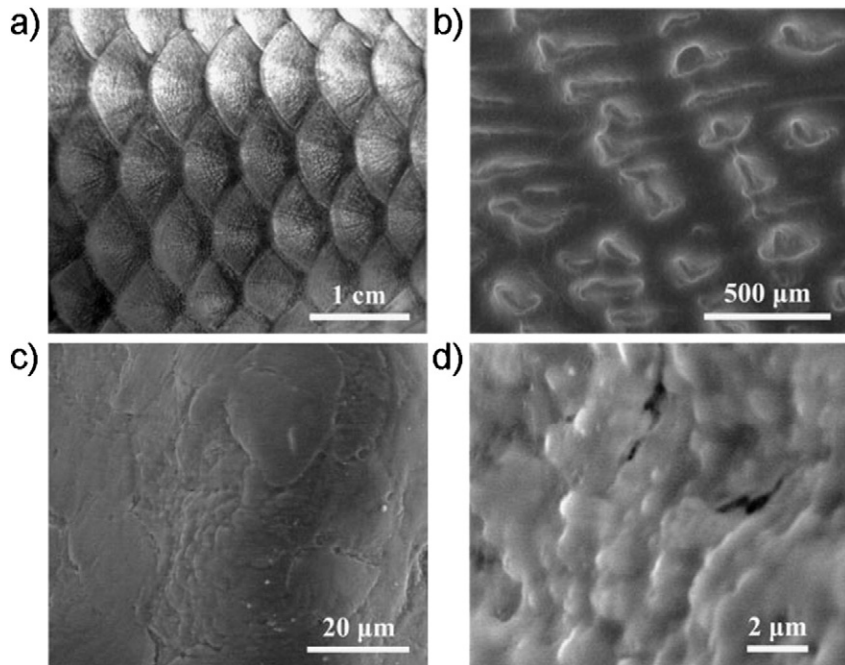


Fig. 7. Surface structures of fish scales. (a) Optical image of the fish scales; (b) SEM image of fish scales; (c) SEM image of the fish scales at high magnification; (d) SEM image of the papillae. Reproduced from reference [51] with permission from Nature Publishing Group.

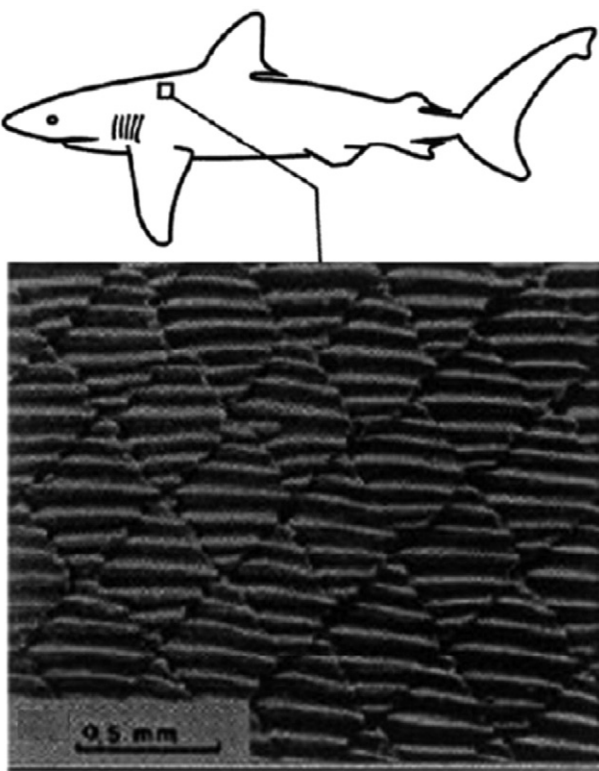


Fig. 8. Scale structure on a Galapagos shark (*Carcharhinus galapagensis*). Reproduced from reference [52] with permission from the Springer.

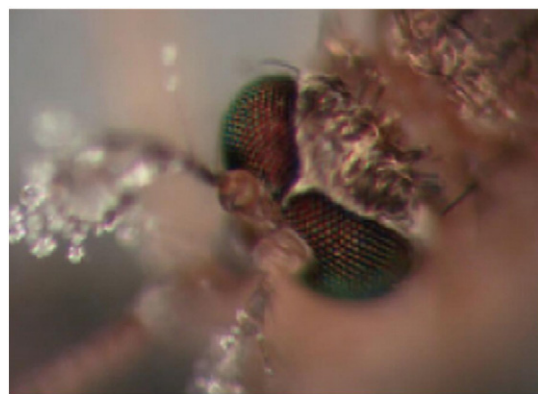


Fig. 10. A photograph of antifogging mosquito eyes. Reproduced from reference [59] with the permission from Wiley.

Rubner et al. have fabricated superhydrophobic/hydrophilic patterned surfaces to mimic the structures on the beetle's back [61]. Water sprayed on superhydrophobic patterns only forms small spherical droplets and is mainly collected on the hydrophilic patterns. Later Garrod et al. also demonstrated the fabrication of superhydrophobic/hydrophilic patterned surfaces to collect water [62]. The water-collecting capabilities of different superhydrophobic/hydrophilic ratios on the surface are investigated in detail in their work. According to the above examples, one can anticipate the future application of superhydrophobic/hydrophilic patterned coatings in practical water collection apparatus.

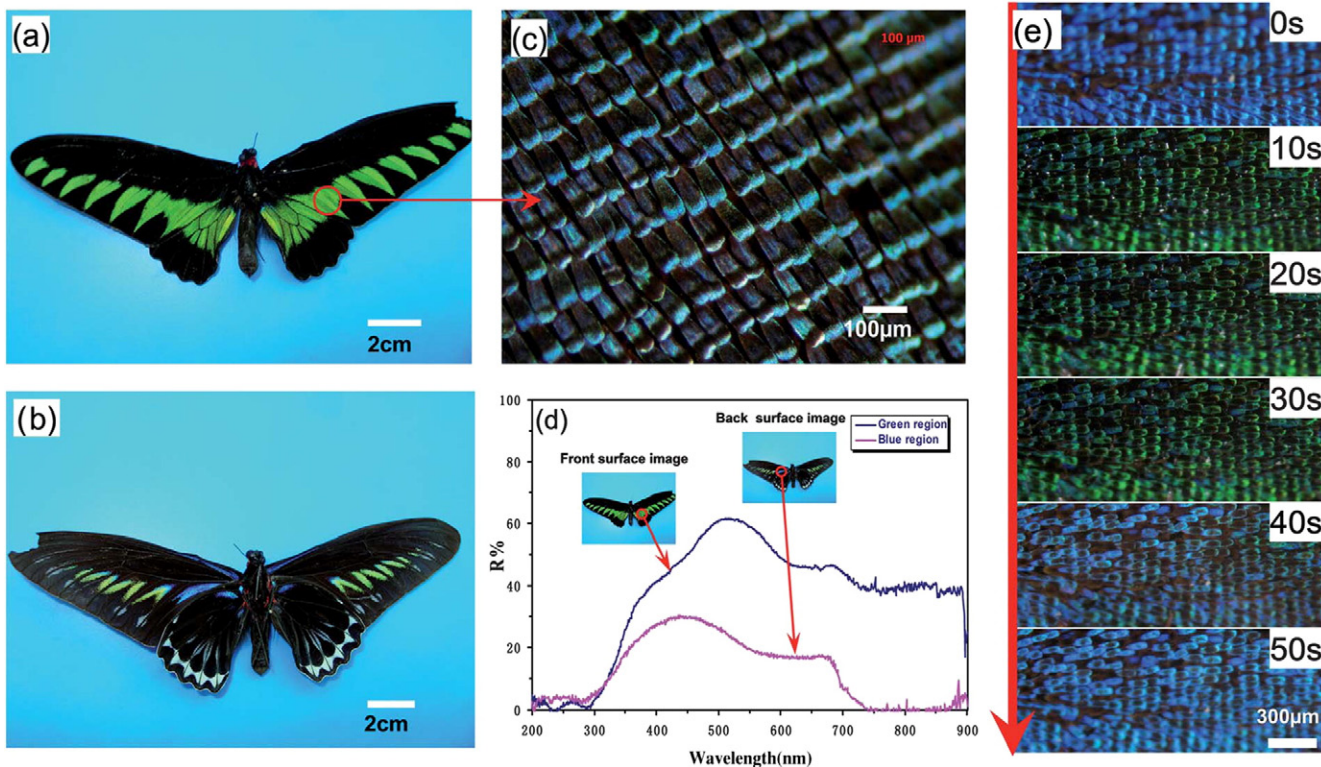


Fig. 9. The appearance and the reflectance spectra of the original wing in butterfly *Trogonoptera brookiana* confirm its light trapping effect. (a) A photograph of the front wing; (b) A photograph of the back wing; (c) Optical microscope image of the butterfly; (d) The reflectance spectra of the scales show a weaker signal in blue region than that in the green region; (e) The one-minute discoloration process shows that the scale color returns to the initial blue color, indicating that the scale color is structure-based. Reproduced from reference [54] with permission from the Royal Society of Chemistry.

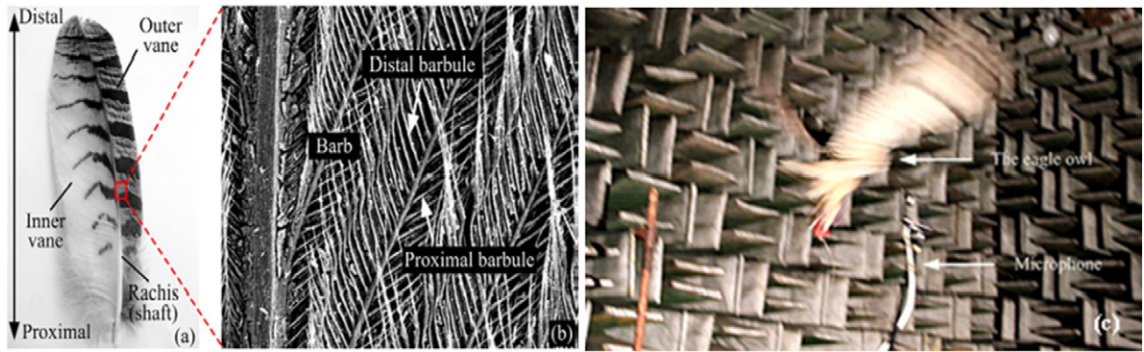


Fig. 11. The wing feather of the eagle owl. (a) The rachis of feather; (b) The barbules grow in different direction; (c) The eagle owl flight noise measurement. Adapted from reference [4] with permission from Elsevier.

3. Modeling and design

3.1. Modeling of self-cleaning for gecko setae

Gecko setae are self-cleaning adhesive. Geckos with dirty feet recovered their ability to cling to vertical surfaces after only a few steps. Self-cleaning occurred in arrays of setae isolated from the gecko. Contact mechanical models suggest that self-cleaning occurs by an energetic disequilibrium between the adhesive forces attracting a dirt particle to the substrate and those attracting the same particle to one or more spatulae. To predict the number of particle-spatula interactions (N) needed to achieve energetic equilibrium with the particle-wall interaction (Fig. 13), researchers [63,64] take the ratio of the interaction energies,

$$N = \left(1 + \frac{R_p}{R_s}\right) \frac{A_{pw} D_{ps}}{A_{ps} D_{pw}} \quad (1)$$

where, R_s and R_p are the radius of gecko spatula and aspherical dirt particle respectively. The p , w and s refer to particle, wall and spatula, respectively. A is the Hamaker constant (typically $\approx 10^{-19}$ J for van der Waals interactions in air). D is the particle-to-wall distance.

In the case of N spatula attached to each particle, approximately half of the particles will remain attached to the wall, and self-cleaning will occur with each step, assuming a clean substrate is encountered. If less than N spatulae are attached to each particle, self-cleaning will occur rapidly as a consequence of energetic disequilibrium; particles tend to remain attached to the wall rather than to the spatula.

3.2. Modeling of superhydrophobic

3.2.1. Modeling of superhydrophobic for water striders

Water striders (*Gerris remigis*) have remarkable non-wetting legs that enable them to stand effortlessly and move quickly on water, a

feature believed to be due to a surface-tension effect caused by secreted wax [65]. But it is the special hierarchical structure of the legs, which are covered by large numbers of oriented tiny hairs (microsetae) with fine nanogrooves, that is more important in inducing this water resistance. According to Cassie's law [66] for surface wettability, such microstructures can be regarded as heterogeneous surfaces composed of solid and air. The apparent contact angle θ_1 of the legs is described by Eq. (2).

$$\cos \theta_1 = f_1 \cos \theta_w - f_2 \quad (2)$$

where f_1 is the area fraction of microsetae with nanogrooves, f_2 is the area fraction of air on the leg surface and θ_w is the contact angle of the secreted wax. Using measured values of θ_1 and θ_w , the air fraction between the leg and the water surface corresponds to $f_2 = 96.86\%$. Available air is trapped in spaces in the microsetae and nanogrooves to form a cushion at the leg-water interface that prevents the legs from being wetted [5].

3.2.2. Modeling of superhydrophobic for gecko feet

The high adhesive forces of gecko feet to water could be explained by the following considerations (Fig. 14a and b). The morphology and orientation of gecko setae are heterogeneous. It is difficult to accurately control the contact modes between gecko spatulae and water droplets. Therefore, researchers came up with two typical solid-liquid contact state, the default state which represents minimizing spatulae contact with water (Fig. 14a), and the adhered state which represents maximizing spatulae contact with water (Fig. 14b). Autumn and Hansen [67] fixed isolated gecko seta arrays on a glass substrate, which can be seen nearly ideal default state arrays, and demonstrate that this array is non-sticky to water. The adhered state, in which the setae are bent so that almost all the spatulae can contact water, contributes the main adhesive force. The origin of the high adhesive force towards water results from high density nanopillars contacting the water. Besides the above

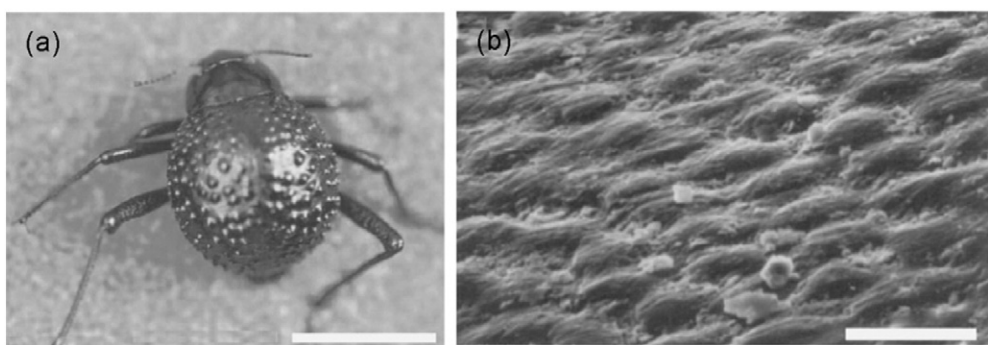


Fig. 12. The water-capturing surface of the fused over wings (elytra) of the desert beetle *Stenocara* sp. (a) Adult female, dorsal view, peaks and valleys are evident on the surface of the elytra; (b) SEM image of the textured surface of the depressed areas. Adapted from reference [60] with permission from Nature Publishing Group.

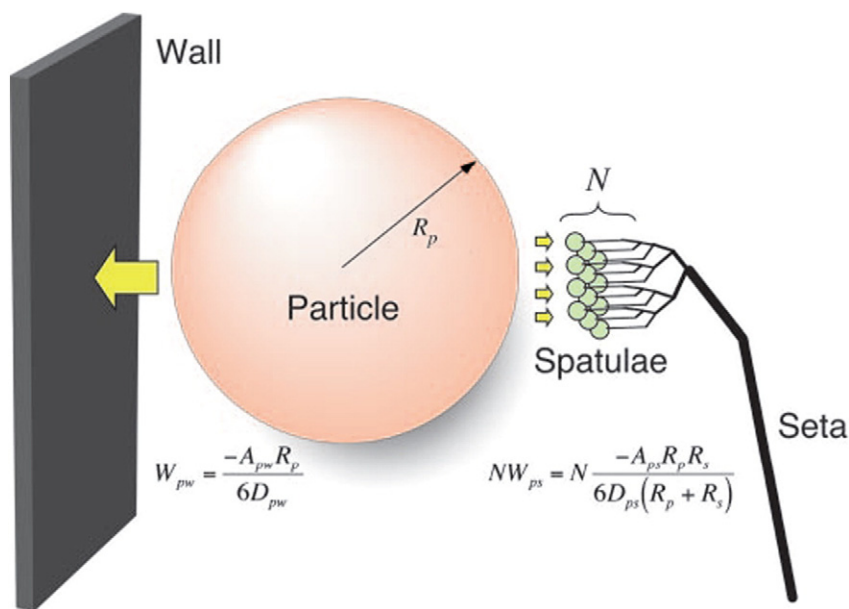


Fig. 13. Model of interactions between N gecko spatulae of radius R_s , a spherical dirt particle of radius R_p , and a planar wall. Van der Waals interaction energies for the particle-spatula (W_{ps}) and particle-wall (W_{pw}) systems are shown. Reproduced from reference [63].

mentioned conformational changes in the surface proteins of gecko setae upon exposure to water, the complex contact condition between water droplets and setae should also be responsible for the wide range of adhesive forces from a low value to a high value [68].

3.2.3. Modeling of directional adhesion of superhydrophobic for butterfly wings

It is known that a droplet tends to slide on the surface of groove microstructures for butterfly wings more easily along the direction parallel to the grooves rather than perpendicular. Two reasonable hypothetical modes were shown in Fig. 15 to clarify the distinct adhesive properties of butterfly wings. When the wing is tilted downward, the micro-scales with ridged nano-stripes are spatially separated from each other and the oriented nano-tips tend to be unwound with flexible micro-scales (Fig. 15a-top). In this case, air can be efficiently trapped in these nano-scale voids among the nano-tips extended by lamellae and the ridged nano-stripes and thus the droplet only touches the top of nano-tips, with a minimal contact area [66]. This ensures the superhydrophobicity of the wings, with a high contact angle above 150°, which has been verified. Moreover, it is known that the ordered arrangement of the micro-structures may influence the contour, length and continuity of three-phase (solid/liquid/gas) contact line and thus control the way a droplet tends to move [69–72]. Accordingly, the ordered arrangement of the micro-scales and nano-stripes on the wings along the radial outward (RO) direction, and the formation of the extremely discontinuous three-phase (solid/liquid/gas) contact line as illustrated in the bottom of Fig. 15a, make the droplet easily roll off the wings along the RO direction.

However, when the wing was tilted upward, the flexible nano-tips and micro-scales take on a close arrangement as shown in Fig. 15b. The nano-tips on the top of the nano-stripes are raised with the flexible micro-scales to closely contact the droplet (Fig. 15b-top). As a result, a quasi-continuous three-phase (solid/liquid/gas) contact line is formed, as shown in the bottom of Fig. 15b when the droplet attempts to move under the gravitational potential against the RO direction. In this case, the pinning at numerous corners (nano-tips) of the steps between the neighboring lamellae on top of the ridged nano-stripes may produce a very high energy barrier, which makes the droplet pin tightly on the wing as it is tilted upward, even when it is fully upright [73].

3.3. Modeling of superoleophobility for fish scales

When the fish scales come in contact with the oil droplets, water molecules can be trapped in the micro/nanostructured fish scales, forming an oil/water/solid interface. This new composite interface shows superoleophobic properties. Although Young's equation [74] was originally applied for a liquid droplet on a solid surface in air, it has also been applied to a liquid droplet on a solid surface in the presence of a second liquid [75,76]. Through Young's equation, we could get the following equation (Fig. 16a):

$$\cos \theta_3 = \frac{\gamma_{11-g} \cos \theta_1 - \gamma_{12-g} \cos \theta_2}{\gamma_{12-g}} \quad (3)$$

where γ_{11-g} is the liquid 1/gas interface tension, θ_1 is the contact angle of liquid 1 in air, γ_{12-g} is the liquid 2/gas interface tension, θ_2 is the contact

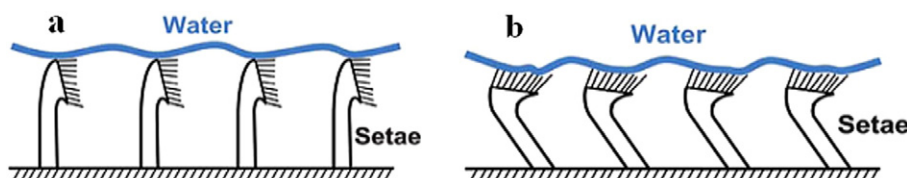


Fig. 14. Schematic of two typical contact states between water droplets and gecko setae: (a) default state and (b) adhered state. Reproduced from reference [68] with permission from the Royal Society of Chemistry.

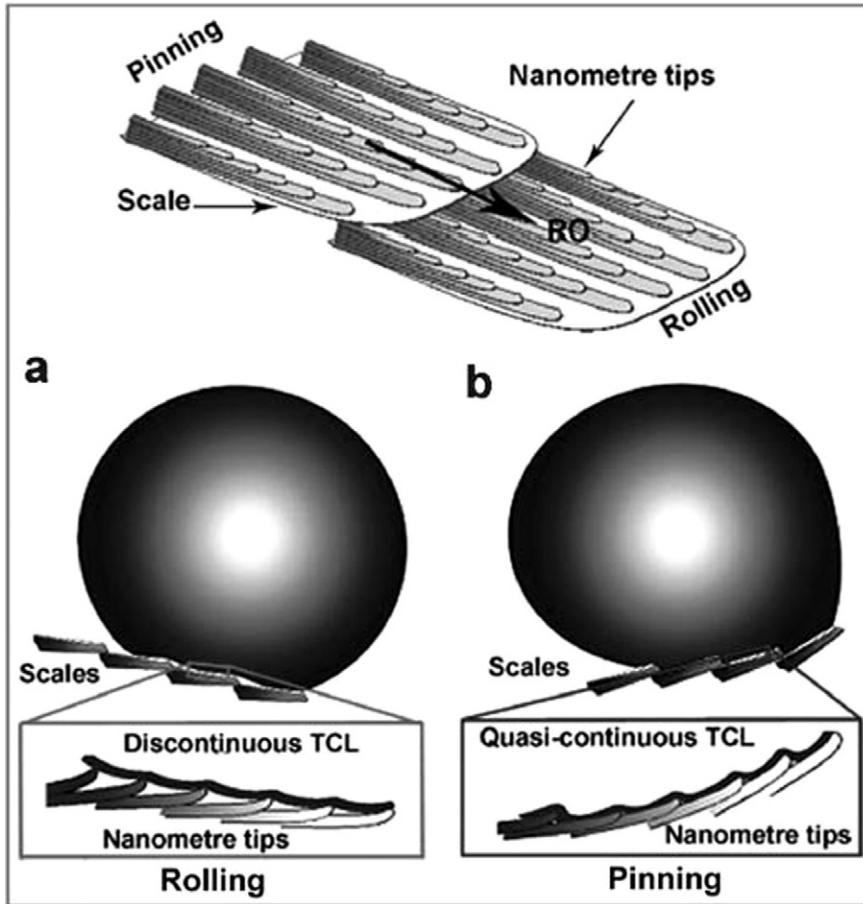


Fig. 15. The models proposed for elucidating the potential mechanism of distinct adhesion dependent on the direction along and against the RO direction. (a) As the wing is tilted down; (b) As the wing is tilted upward. Reproduced from reference [73] with permission from the Royal Society of Chemistry.

angle of liquid 2 in air, $\gamma_{l_2-l_1}$ is the liquid 1/liquid 2 interface tension, and θ_3 is the contact angle of liquid 1 in liquid 2. Using Eq. (3), it was able to explain why a hydrophilic surface in air becomes oleophobic in water.

For a rough surface composed of solid and air, Cassie et al. [66] proposed a model describing the contact angle in a water/air/solid system. In an oil/water/solid system, on the other hand, where the rough surface is composed of solid and water (Fig. 16b and c), the Cassie model is expressed as follows [49]:

$$\cos \theta'_3 = f \cos \theta_3 + f - 1 \quad (4)$$

where f is the area fraction of solid, θ_3 is the contact angle of an oil droplet on a smooth surface in water, and θ'_3 is the contact angle of an oil droplet on a rough surface in water (the area fraction f).

Because the area fraction f is contact angle 0.5 in a microstructure silicon surface, it could calculate $\theta'_3=148.5^\circ$ according to Eq. (4). For a

micro/nano-structured silicon surface, f is close to 0. So, θ_3 is close to 180° according to Eq. (4) [49].

3.4. Modeling of frictional adhesion

Geckos are easily and rapidly able to climb. Models of peeling tape generally treat the adhesive surface as a continuum. The force during peeling of a flexible strip of tape is given by [77]:

$$F = bdE \left(\cos \alpha - 1 + \sqrt{\cos^2 \alpha - 2 \cos \alpha + 1 + 2R/dE} \right) \quad (5)$$

where b is the width of the strip, d is the thickness of the strip, E is material stiffness, R is the adhesion energy, and α is the peel angle. Consider a weight suspended from a strip of tape attached to a surface of angle

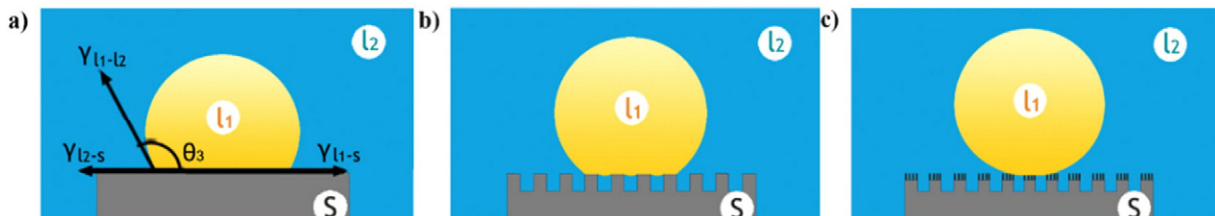


Fig. 16. Effect of surface structure on the wetting behaviors of solid substrates in solid/oil/water three-phase systems. (a) Diagram of Young's equation at the condition of a liquid 1 droplet on a smooth surface with a contact angle θ_3 in a liquid 2 phase; (b) An oil droplet on a microstructure substrate in water, in which /1 represents oil and /2 represents water; (c) Same system on a micro/nanostructured substrate. Reproduced from reference [49] with the permission from Wiley.

α over vertical. Solving for α in Eq. (5), the angle (α^*) at the onset of peeling is obtained by Eq. (6):

$$\alpha^* = \cos^{-1} \left(1 - \frac{bR}{F} + \frac{F}{2bdE} \right) \quad (6)$$

The peeling model predicts that greater weight will initiate peeling at shallower angles. Including the elastic stretch term, maximum peeling force, which occurs at low angles, is limited by some factor in Eq. (7):

$$F_{\max} = \sqrt{2Rb^2dE} \quad (7)$$

where b is the width of the strip, d is the thickness of the strip, E is material stiffness, R is the adhesion energy, F_{\max} is the maximum peeling force.

Showing that stiffer materials, given the same adhesion energy, it will peel at higher loads. Peeling mechanics can be applied—at least in theory—to fibrillar gecko-like materials [78]. However, in real geckos where attachment is via a series of scissors bearing anisotropic setae, the validity of conventional peeling mechanics is less clear. Geckos hold their toes in a hyperextended position when not climbing—possibly protecting the scissors from abrasion, suggesting that digital hyperextension could have functions other than reduction of detachment force via peeling mechanics. Indeed, it has been suggested that spatulae could detach more or less simultaneously [79], due to their mechanical independence. When dragged against their natural path (against curvature) setal arrays remained compressed and did not adhere (Fig. 17a). When dragged along their natural path (with curvature) setal arrays compressed initially and then adhered, resulting in tensile normal forces (Fig. 17b).

3.5. Modeling of light trapping

A structural model was built to mimic the butterfly scale absorbing solar heat. The array of scales plays the role of a very efficient optical diffuser of the visible range. It is assumed that in shelf microstructure the low reflectance is due to alternating layers of air and chitin, which can cause reflection, transmission and absorption at each interface (Fig. 18a and b). The thickness of each layer determines what wavelength will be reflected and of these, what will constructively or destructively interfere at specific viewing angles [80]. In this case, the arrangement of the layers induces interference destructively, and consequently most of the solar energy is absorbed by chitin layers after multi-absorption. As for the quasi-honeycomb-like microstructure, micro-diffraction gratings are formed with periodic parallel slits or grooves on the magnitude of the light wavelength [80] and the tiling of these micro-gratings generates a quasi-honeycomb-like structure (Fig. 18c and d) that can diffract incident light into the scales to be absorbed. Whenever the light meets another part of the surface after it enters the scale, it is reflected back into the material, embracing the second reflection, and consequently, it will be reflected multiple

times. The structural color exhibited by the wing is determined by the position of the reflectivity peak, which can be verified by the adjusted Snell's law [3].

$$N\lambda = 2d \left(n_{\text{eff}}^2 - \sin^2 \theta \right)^{1/2}, N = 1, 2, 3, \dots \quad (8)$$

where d is the single lattice constant, λ is the wavelength, θ is the incidence angle and N is an integer. n_{eff}^2 is the effective refractive index which is determined by the relative refractive index of different materials, and shown by the following function:

$$n_{\text{eff}}^2 = n_1^2 f_1 + n_2^2 (1 - f_1) \quad (9)$$

One lattice had two kinds of materials: cuticula and air. n_1 and n_2 represent the refractive index of cuticula and air, respectively. f_1 is the spacing ratio of the lattice, namely equal to $a/(a + b)$. a and b is the thickness of the cuticula and the air film, respectively. As a result, almost all the incident light ends up adsorbed by the scale.

3.6. Modeling of fluid-drag reduction

The fact that ribbed surfaces (riblets) aligned in the stream-wise direction do reduce turbulent skin friction has been established beyond any reasonable doubt [52]. Representative model of shark surface morphology includes triangular, parabolic, blade shape, and their cross-sectional diagrams are as shown in Fig. 19. The triangular has the best characteristics of drag reduction. Luchini [81] believed when the relationship between height and width is $h \geq 0.6 s$ (where h and s refer to the height and width of a riblet, respectively), the fluid resistance is the smallest. Bechert [52] used adjustable height of the riblet in the pipeline for test. The result showed that the best riblet height should be $h = 0.5 s$. Meanwhile, adhesion resistance of the riblet surface was reduced by 9.9% than that of the smooth surface [82]. The drag reduction effect was worse as height of riblet increasing when $h > 0.6 s$.

3.7. Modeling of erosion resistance

Desert scorpion (*Androctonus australis*) is a typical animal living in sandy deserts, and may face erosive action of blowing sand at a high speed [25]. Bionics study shows that some special morphologies of the organism surface always exhibit excellent functions. The four patterns of bionic models for desert scorpion are shown in Fig. 20. Fig. 20a shows the convex pattern bionic model, many convex domes distribute on the material surface. The influencing factor of the erosion resistance of this model is the distribution of the convex domes, which contains the radius and the height of the dome, and position distribution of the center coordinates of the domes. Fig. 20b shows the groove pattern bionic model, many grooves are excavated on the material surface, and the grooves are parallel to each other, the feature of the cross-section is arched structure. The influencing factors of the erosion resistance of

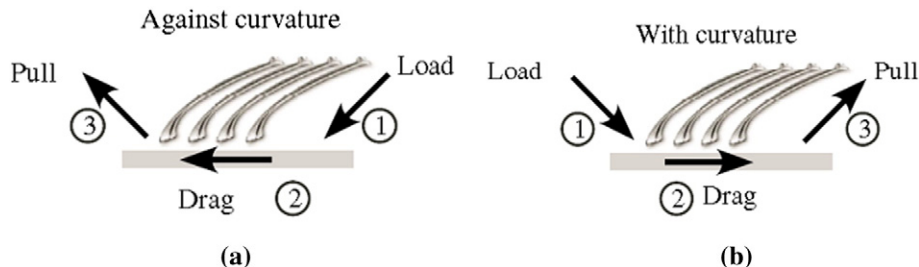


Fig. 17. Shear and normal forces in isolated gecko setal arrays on a glass surface. (a) Setal array during load (1), drag (2) and pull (3) (LDP) against the curvature of the setal shafts exhibits Coulomb friction; (b) Setal array during LDP with the curvature of the setal shafts compressed initially, and then was pulled into tension as the setal tips adhered. Reproduced from reference [77].

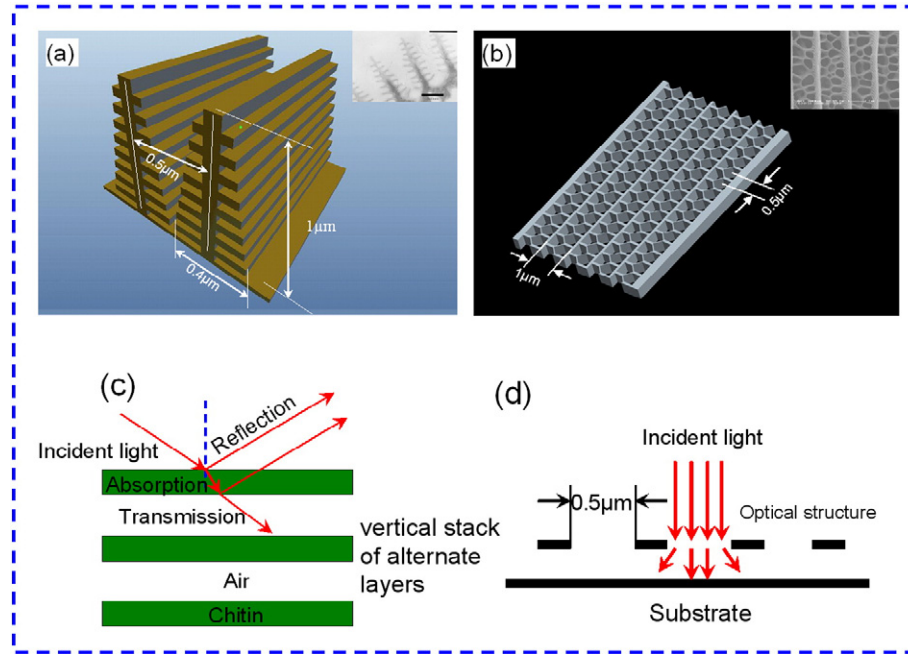


Fig. 18. 3D single scale models of (a) shelf structure and (b) quasi-honeycomb-like structure. (c) The optimized vertical stack of alternate layers of air and chitin is the interpretation of the mechanism of the multiple absorption, and the mechanism of the light trapping effect of the quasi-honeycomb-like structure is explained appropriately by (d) the diffraction at the interface. Reproduced from reference [54] with permission from the Royal Society of Chemistry.

this model are the depth and width of the groove, and the spacing between each two grooves.

The erosion resistance performance of the dorsal surface of scorpion is not only related to the special surface morphology, but also attributed to multiple factors coupling function. The domes and grooves on the surface are morphological coupling elements, and the flexible connection is flexible coupling element. The coupling bionic model is built by combining the coupling elements, and the coupling bionic models are shown in Fig. 20c. The flexible connection of the model was removed, and divided into two layers. The upper layer is hard material and processed into bionic surface morphology, and the lower layer is flexible materials. The two-layer structure forms a soft and hard alternated composite structure, as shown in Fig. 20d.

4. Fabrication approaches

Fabrication of biomimetic multi-functional surface structures inspired from animals employs various methods which can be roughly classified into two types: chemical routes and physical routes.

4.1. Chemical routes

4.1.1. Sol-gel

Sol-gel process involves hydrolysis of the sol and drying to form a gel. For a good reproduction of natural surface structures inspired from animals, a liquid precursor is favorable [83]. It mainly uses the metal alkoxides to prepare the inorganic materials. It provides a new way of tailoring and controlling the microstructure of materials through a low temperature chemical method.

With sol-gel approach, multi-functional micro/nano-surfaces can be prepared without any assistance from photolithography, laser lithography and other expensive technologies. For example, Zhang et al. [84] developed a novel natural stamp, the outward wings of grasshoppers (OWG), for making anisotropic surfaces. The two-step replica exhibited anisotropic high hydrophobicity and light reflection. Fig. 21 shows the schematic representation of the two-step replication process using sol-gel and the images of the positive and negative replicas. The results proved that an anisotropic wetting surface was achieved by duplicating the surface structure of OWG.

The most useful method to coat small materials with inorganic materials is sol-gel coating carried out in aqueous media [85]. In typical sol-gel coating, inorganic sol particles undergo surface preferred gelation to form an inorganic coat on the templates. However, examples of coating biological materials by sol-gel coating are rare [86]. This is probably because most biological materials are negatively charged at moderate conditions, which is not ideal for sol-gel coating that is accomplished by taking advantage of electrostatic attraction between negatively charged sol particles and positively charged templates. Also, the ashes from biological materials could also disturb the formation of replicas in this method. In this regards, Kim et al. have recently reported interface-selective sol-gel polymerization that was useful to coat different templates regardless of charges on them [87]. Reaction conditions in that method were so mild that living microorganisms were coated without being sacrificed [88].

Notably, some smart hydrogel, prepared by sol-gel process, has a reversible swelling and de-swelling property with volume transition and has been applied in drug delivery, biosensors, and bioelectronics including tunable personal computers. With the hope to expand or shrink the natural species' inner structures, Zang et al. used an electric field

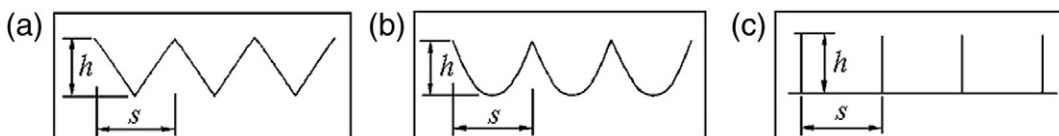


Fig. 19. Model of shark surface morphology (a) triangular, (b) parabolic and (c) blade shape. Reproduced from reference [82].

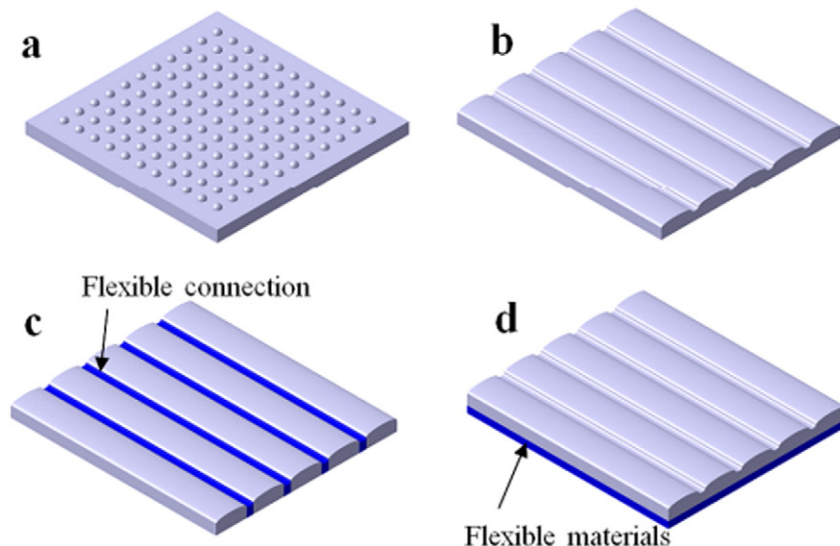


Fig. 20. Bionic modeling of desert scorpion back. (a) Convex pattern; (b) Groove pattern; (c) Coupling bionic models with flexible connection; (d) Coupling bionic models with soft and hard alternated composite structure. Adapted from reference [25] with permission from the American Chemical Society.

sensitive hydrogel (EFSH) to embed and fill the wing scales of sunset moth with rich structural colors [89]. The EFSH swelled and deswelled with volume transition that modified the structures of wing scales, resulting in materials' reflectance peak shift for visible light. The CTS/PVA/moth wing scale composites, prepared by the steps described in Fig. 22, responded effectively and stably to the electric field, heat, and air pressure, showing a reversible multi-responding property to various external stimuli.

In addition, there are few reports that combine the unique multi-functional surface structures of animals with the intrinsic properties of the replica materials, even though this is one of the most important objectives of biomimetication. Zhang et al. conducted some works that ZnO replicas with photonic structures were obtained via a sol-gel bio-template method. The dark black (DB) wing scale replicas exhibit a photonic band gap (PBG) in the visible region, which overlaps with the visible emission range of ZnO [90].

When using sol-gel process to produce biomimetic materials, an impregnation or infiltration of the templates is an important step. For

example, Cook et al. observed an incompatibility between butterfly wing and the silane coating, which led to catastrophic cracking of the coating during calcinations [91]. Zhang et al. avoided this problem by choosing a zinc nitrate water-free ethanol solution as the precursor, based on the knowledge that butterfly wing surface contains chitin with functional groups that act as centers to absorb Zn(II) by hydrogen bonding, thus zinc ions could soak the template well [92]. ZnO replicas exhibiting the fine wing-scale features were obtained, as a result of good compatibility between template and the precursor.

In summary, the sol-gel method is very suitable considering its advantages like chemical flexibility, facile shape control, and mild reaction conditions. When using a sol precursor to produce biomimetic materials, impregnation or infiltration of the templates is an important step. A good wetting between the sol and the template is crucial for the final product to preserve morphology, fine features, properties and functions [93] of the template [83]. In another hands, there are also many problems for the sol-gel. Generally, the raw materials are relatively expensive and harmful to health. There are also some large

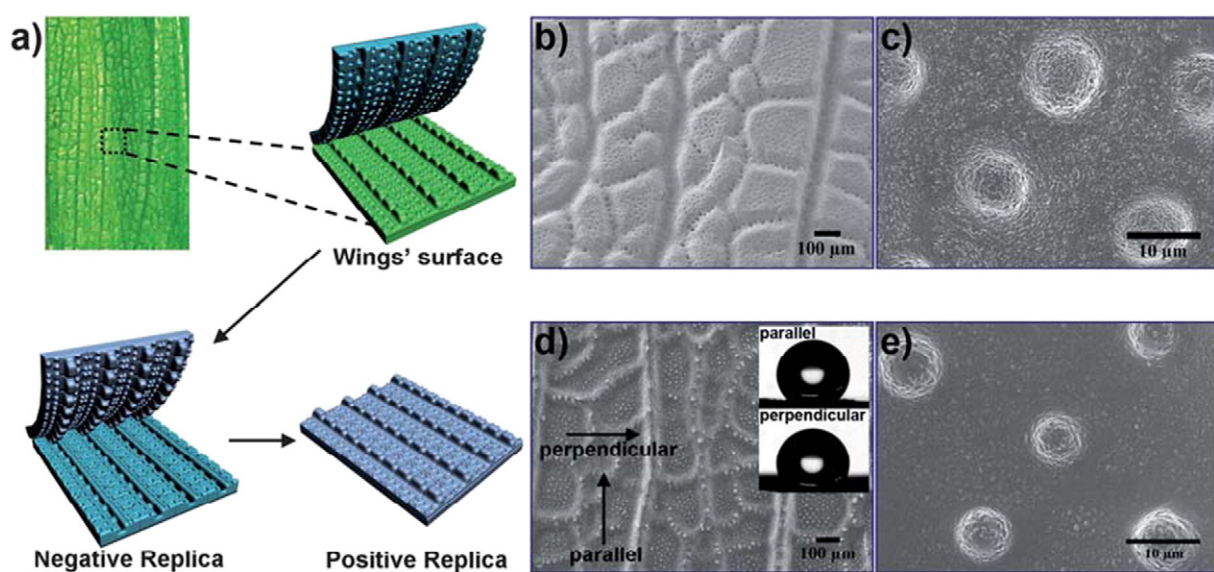


Fig. 21. (a) Schematic representation of the two-step replication process using sol-gel; (b, c) SEM images of first-step PDMS replica of the outward wings of grasshoppers; (d, e) SEM images of second-step PDMS replica of the outward wings of grasshoppers. Inserts in (d): Anisotropic high hydrophobicity of second-step PDMS replica. CA is $137.8^\circ \pm 4.7^\circ$ measured from the parallel direction and $109.5^\circ \pm 4.1^\circ$ measured from the perpendicular direction. Reproduced from reference [84] with permission from the Royal Society of Chemistry.

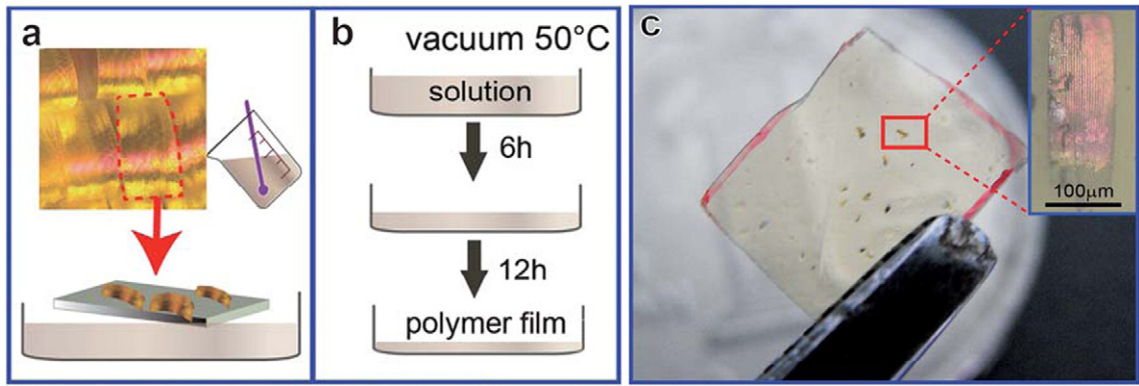


Fig. 22. (a), (b) Preparation of CTS/PVA/wing scale composites; (c) Obtained composite with wing scales buried in the CTS/PVA hydrogel. Inset: Optical microscope image of an embedded wing scale. Reproduced from reference [89] with permission from the Royal Society of Chemistry.

pores in the gel material. A certain amount of gas will escape out from the gel material during the drying process, resulting in structural contraction.

4.1.2. Etching

When using etch process to produce sub-wavelength structures (SWSs), the parameters of etching and dewetting processes is crucial for the antireflective property of SWSs. For example, Leem et al. [94] have theoretically and experimentally investigated the influence of the process parameters on the antireflective properties of disordered Si SWSs using the Pt thin films as the etch mask and subsequent ICP etching in SiCl_4/Ar plasma. The geometric profile and antireflective property of the fabricated Si SWSs were strongly dependent on the thermally dewetted Pt nanopatterns and various etching parameters. It was found that the Si SWS with more tapered shape and higher height using the completely dewetted dot-like Pt nanomask pattern yielded a relatively low reflectance.

Recently, antireflective structures (ARS) surfaces on silicon prepared by nano sphere lithography have been reported [96], but there are few ARS surfaces on fused silica or on non-planar lenses. So, Li et al. have demonstrated a versatile and time efficient method to fabricate large area fused silica cone arrays on planar fused silica substrates and plan convex lenses for high performance antireflective and antifogging surfaces [95]. A schematic representation of the fabrication process of ARS surfaces is illustrated in Fig. 23. The silica cone arrays were prepared by a short time reactive ion etching (RIE) using 2D polystyrene (PS) colloidal crystals as masks. In another study, they also demonstrated a simple method to improve the light extraction of white organic light emitting diodes (OLEDs) by silica biomimetic antireflective

surfaces. A non-close-packed hexagonal silica cone array was directly etched on the opposite side of the indium-tin-oxide (ITO)-coated fused silica substrate. This method mentioned here can be introduced in any OLEDs without any alteration of device structure and materials design [97]. In addition, a two-dimensional sub-wavelength grating (SWG) has been fabricated on a GaAlAs light emitting diode (LED). The SWG is patterned by electron beam lithography and etched by fast atom beam with Cl_2 and SF_6 gases [98].

Etching is one kind of extremely important step of the semiconductor manufacturing process, microelectronics IC manufacturing process and micro-nano manufacturing process. It is also one of the main craft of graphical processing, associating with photolithography. First, through the photolithography, photoresist is exposed by lithography treatment and then, by other ways, the etching removal treatment is realized and the part of the removed off is removed. Along with the development of the micro-fabrication process, generally speaking, etching is a general designation of detaching or removing material through a solution, a reactive ion or other mechanical approach, becoming a universal way of micro processing and manufacturing. At the same time, this process has some obvious shortcomings. The thickness of the structure in nanoscale is extremely difficult to control. So, it is difficult to obtain highly ordered nanostructures when directly using this process to manufacture nanostructures.

4.1.3. Sonochemical

Sonochemical methods utilize the energy of sonication to promote chemical reactions for material production. For the first time, the fine hierarchical structures of butterfly wing were successfully duplicated in manganese oxide using sonochemical reduction followed by calcination

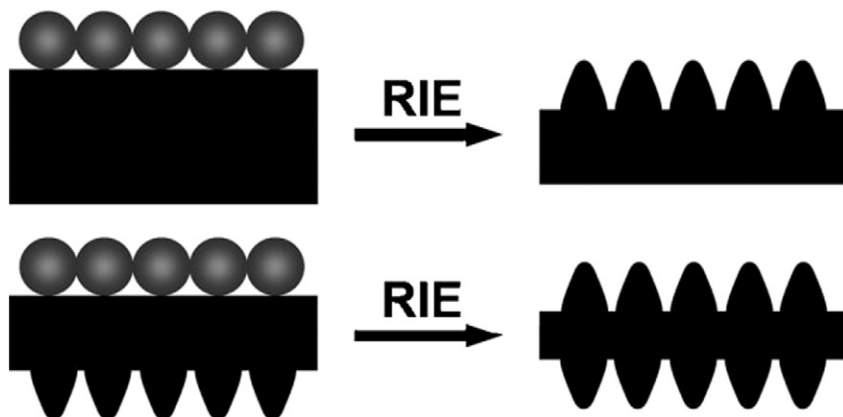


Fig. 23. Schematic illustration of the process for preparing ARS surfaces. Reproduced from reference [95] with the permission from Wiley.

[99]. The morphologies and surface structural details of the original butterfly wing and the calcined Mn_2O_3 butterfly wing are compared in Fig. 24. New functional materials with chosen hierarchical structures of biotemplates combined with the functionality of metal oxides could be synthesized in the future by the sonochemical method presented in this work [99].

This method for fabricating hollow nanostructures is simple, low-cost and energy-conserving. It can be extended to fabricate hollow nanostructures of various morphologies with bacteria of other shapes as templates, e.g. vibrios, spirillum, square bacteria, fusiform bacilli. Since sonochemical methods can produce many attractive materials, biomimetic mineralization under sonochemical conditions can be extended to these materials for the synthesis of their hollow nanostructures, multi-scale structures, and so on [83].

4.1.4. Chemical vapor deposition (CVD) and chemical vapor infiltration (CVI)

Chemical vapor deposition (CVD) is a process that deposits materials on a surface using gaseous reactants. CVD is employed for biomimetic mineralization with the advantages of flexible chemistry and near net-shaping. CVD is generally used to fabricate metal and non-metallic films. It can also fabricate multi-component alloy film. However, the temperature in the CVD process is high (100 °C), which severely limits the scope of their application. Cook et al. produced SiO_2 replicas of butterfly wings and housefly wings using CVD [91]. The replicas well retained delicate features of the original templates. While CVD deposits materials onto a surface, chemical vapors in chemical vapor infiltration (CVI) can penetrate porous structures and deposit materials within the "body". Most materials that can be deposited by CVD can also be deposited by CVI [83].

In another example, Watanabe et al. have fabricated a *Morpho*-butterfly-scale quasi-structure using focused-ion-beam chemical-vapor-deposition (FIB-CVD) and observed brilliant blue reflection from this quasi-structure with an optical microscope for the first time [100]. They successfully demonstrated that a *Morpho*-butterfly-scale quasi-structure fabricated by FIB-CVD can show nearly the same optical characteristics as real *Morpho*-butterfly scales.

On one hand, in the CVD and CVI, the gaseous reactants with good flowing properties could be employed. So, the complex structures of the templates can be replicated with near net-shaping. Besides, CVD and CVI could achieve control of the coating thickness by varying the number of deposition or infiltration cycles, and there is no background deposition, which may occur in wet chemical methods like sol-gel and precipitation [83]. Despite the many different advantages, CVD and CVI are relatively expensive methods. The deposition rate of CVD

is also not too high, generally several hundreds of nanometer per minute. When using this method to produce the biomimetic multi-functional surface of animals, the required temperature in CVD and CVI often higher than that of carbonization of organic matter. So, the CVD and CVI are greatly restricted, especially for the organic material substrate.

4.1.5. Atomic layer deposition (ALD)

Atomic layer deposition (ALD) is a thin film growth technique that uses alternating and saturating reactions between gaseous precursor molecules and a substrate to deposit films in a layer-by-layer fashion [101]. Al_2O_3 replicas of butterfly wing scales with well-controlled coating thickness were also produced through ALD [102]. Wing scales coated with a 10-, 20-, 30-, and 40-nm thick Al_2O_3 layer were obtained by varying the cycles of deposition, and their reflected colors shifted from original blue to green, yellow, orange, and eventually pink in optical microscopic imaging. This red-shift was due to the surface-film-enhanced reflection of a particular wavelength determined by the thickness and refraction index of the film. In another study, Kolle et al. used a combination of layer deposition techniques (Fig. 25), including colloidal self-assembly, sputtering and atomic layer deposition, to fabricate photonic structures that mimic the color mixing effect found on the wings of the Indonesian butterfly *Papilio blumei* [103]. They also showed that a conceptual variation to the natural structure leads to enhanced optical properties.

Among a variety of deposition methods, ALD offers a unique capability of control over the final pore size and thickness of the deposited layer with atomic-layer precision [104], which makes it an attractive method for producing precise and conformal coatings over nanoporous materials. The material flexibility of ALD, as well as its capability of control over the coating thickness, and hence dimension of the fine structures (like pore sizes), with atomic layer precision, makes ALD an intriguing method for fabricating materials with desired and controllable properties. It can be simply achieved precisely control of the film thickness through controlling the response cycle number of ALD. The film thickness can be achieved control in atomic-level. Despite the many advantages, ALD are also relatively expensive methods than CVD and CVI. The deposition rate of ALD is extremely slower than CVD and CVI, because the deposition is carried out in atomic monolayer film.

4.1.6. Assembly methods

Assembly processes involve attractive and repulsive interactions between building blocks, and building block interactions with solvents, interfaces and templates. At the molecular level, the driving forces for the assembly are usually chemical, which can be ionic, covalent, hydrogen, non-covalent, metal-ligand bonding interactions, etc. At scales beyond

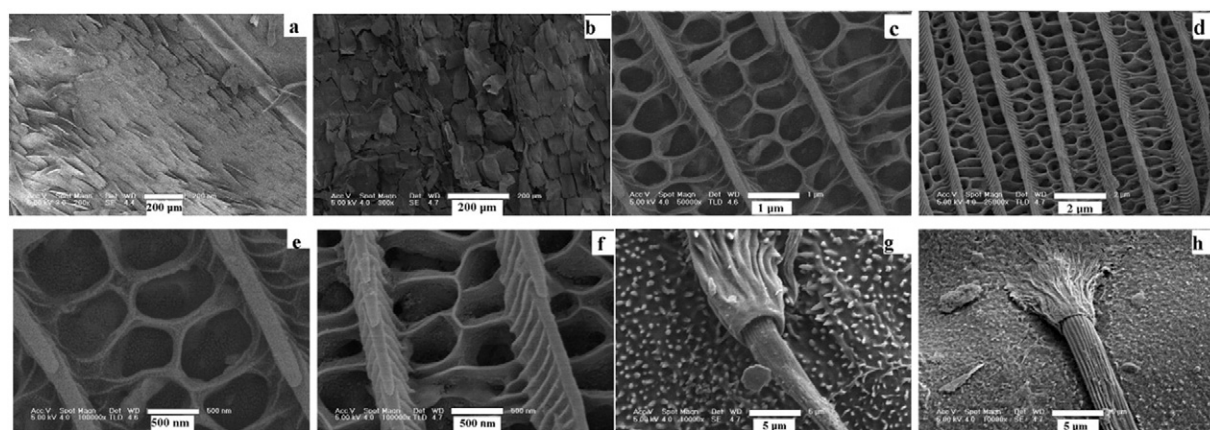


Fig. 24. FE-SEM images of *Graphium sarpedon* (a, c, e) butterfly wing and (g) peg-and-socket attachments and of calcined replica Mn_2O_3 (b, d, f) butterfly wing and (h) peg-and-socket attachments. Adapted from reference [99] with permission from the American Chemical Society.

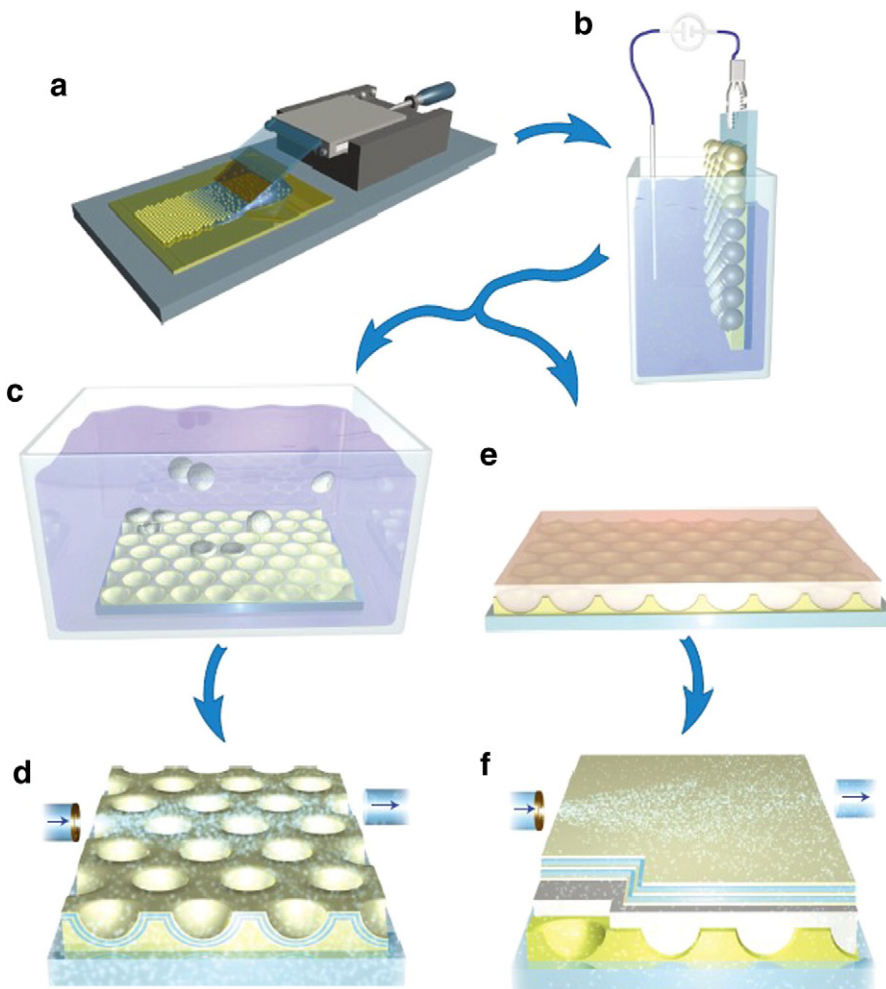


Fig. 25. Sample fabrication. (a) Deposition of polystyrene colloids on a gold-coated silicon substrate; (b) Growth of platinum or gold in the interstices of the colloidal array by electroplating. The metal deposition is terminated when the thickness of the deposited film equals the microsphere radius; (c) Removal of the polystyrene spheres from the substrate by ultrasonication in acetone; (d) Sputtering of a thin carbon film and ALD of a stack of 11 alternating TiO_2 and Al_2O_3 layers (arrows indicate the precursor gas flow); (e, f) In a second route, the colloids are molten to cover the cavities with a homogeneous film (e) which is covered by a TiO_2 - Al_2O_3 multilayer (f). Reproduced from reference [103] with permission from Nature Publishing Group.

the molecular forces for materials self-assembly are usually physical, including capillary, colloidal, elastic, electric, magnetic, and shear. For example, some researchers reported a simple yet scalable self-assembly technique for fabricating efficient moth-eye antireflection coatings with adjustable reflectivity and non-close-packed microstructures, which were not easily available by traditional self-assembly approaches [105]. Wafer-scale, non-close-packed colloidal crystals with remarkable large hexagonal domains were created by a spin-coating technology.

Assembly is generally carried out in aqueous environments, because good mobility of the preformed nanoparticles is favorable for the formation of a structure with high integrity. The preformed nanoparticles are usually prepared in the form of a colloid or a suspension. This method requires relatively high and complex external conditions and is vulnerable to outside factors, including molecular recognition, structure and number of components, nature and composition of the solvent. Self-assembly is the only practical approach for building a wide variety of nanostructures. Making sure the components assemble themselves correctly, however, is not an easy task. Because the forces at work are so weak, self-assembling molecules can get trapped in undesirable conformations, making defects all but impossible to avoid. Any new system that relies on self-assembly must be able either to tolerate those defects or repair them [106].

4.2. Physical routes

4.2.1. Physical evaporation and deposition

Evaporation and deposition can reproduce fine structures of bio-templates [83]. In one study, Chung et al. fabricated a *Morpho*-mimetic thin film by depositing a dielectric multilayer on top of a silica microsphere base layer with a random size distribution. Such a combination induces a spontaneous emergence of both order and disorder across many length scales without any lithography or complicated fabrication process. This enables us to fabricate, at a large scale, thin films that not only reproduce the bright, brilliant glossy colors comparable to *Morpho rhetenor* butterflies, but actually outperform both *Morpho rhetenor* and *Morpho didius* butterflies in maintaining their color and brightness over a wide range of viewing angles in ambient conditions [107].

Physical evaporation and deposition is a straightforward method to replicate surface features of the underlying substrates through forming a thin coat. Thickness of the coating can be controlled by the number of deposition cycles, but fine surface features may be lost if the coating is too thick.

4.2.2. Imprinting

Imprinting is an exciting method among structure-cloning technology of microelectronics devices. For example, Ho et al. presented an

antireflective structure consisted of irregular nanopillars to increase light extraction efficiency of flexible organic light-emitting devices. The nanopillars were made by imprinting the anodized aluminum oxide on polycarbonate substrates. With the nano-imprinted irregular and tapered nanopillars on the PC film, a high-performance AR layer was made. The AR layer simultaneously increased the image contrast ratio and light extraction efficiency [108].

Using inkjet printing, Kang et al. showed the ability to infuse fine droplets of silicone oils into the crystal, locally swelling it and changing the reflected color. They have demonstrated the use of self-assembled colloidal photonic crystal substrates to support high resolution, multi-color, stable but erasable images printed with transparent silicon oils of varying molecular weight (Fig. 26) [109].

This method will pressure cavities or template onto the conformal materials. Then the materials will be deformed in accordance with the template graphics. Finally, the graphics of template will be copied onto the materials through the UV exposure or heat treatment method. Comparing with most of the traditional microelectronics manufacturing process, imprinting technology not only can copy graphics on XY direction, but also it can press the steps of the profile of structure in vertical direction. For the microscale fabrication technologies, imprinting is a potentially broad range of applications on manufacturing the multi-functional surface structures of animals.

4.2.3. Direct laser writing

There are many types of direct-write techniques used in science and engineering [111]. In the most classical sense, engraving or milling can be considered a direct-write process, since a tool or stylus makes contact with a surface and moves in a desired pattern to produce a feature. The coupling of a high powered laser with direct-write processing enables similar features to be produced without requiring physical contact between a tool and the material of interest. Because of this, few techniques share the versatility of laser direct-write (LDW), in adding, subtracting, and modifying different types of materials over many different length scales, from the nanometer to the millimeter scale.

Turner et al. showed the fabrication and characterization of a novel class of biomimetic photonic chiral composites inspired by a recent

finding in butterfly wing-scales. They employed the direct laser writing method, which provided the ability to realize 3D microstructures with arbitrary geometry. The 3D networks were written by the 3D translation of the photoresist mounted on a piezoelectric translation stage. A key feature of the structural design is that the overall microstructure is in the shape of a pyramid with a flat top, analogous to cleaving the boundaries along the crystallographic planes. They also had experimentally and numerically characterized the transmission spectra of these microstructures showing strong circular dichroism within these chiral composites [112].

From the earliest work on laser interactions with materials, direct-write processes have been important and relevant techniques to modify, add, and subtract materials for a wide variety of systems and for applications such as metal cutting and welding. In general, direct-write processing refers to any technique that is able to create a pattern on a surface or volume in a serial or “spot-by-spot” fashion. This is in contrast to lithography, stamping, directed self-assembly, or other patterning approaches that require masks or preexisting patterns. At first glance, one may think that direct-write processes are slower or less important than these parallelized approaches. However, direct-write allows for precise control of material properties with high resolution and enables structures that are either impossible or impractical to make with traditional parallel techniques. Furthermore, with continuing developments in laser technology providing a decrease in cost and an increase in repetition rates, there is a plethora of applications for which (LDW) method is a fast and competitive way to produce novel structures and devices.

4.3. Template removal

Following biomorphic mineralization, templates can be removed to yield inorganic materials, while sometimes the templates are allowed to remain and form inorganic/organic composites. There are several ways for removing the template, if its removal is desired.

Papilio paris butterflies have an iridescent blue color patch on their hind wings which is visible over a wide viewing angle. Optical and scanning electron microscopy observations of scales from the wings show that the blue color scales have very different microstructure to the

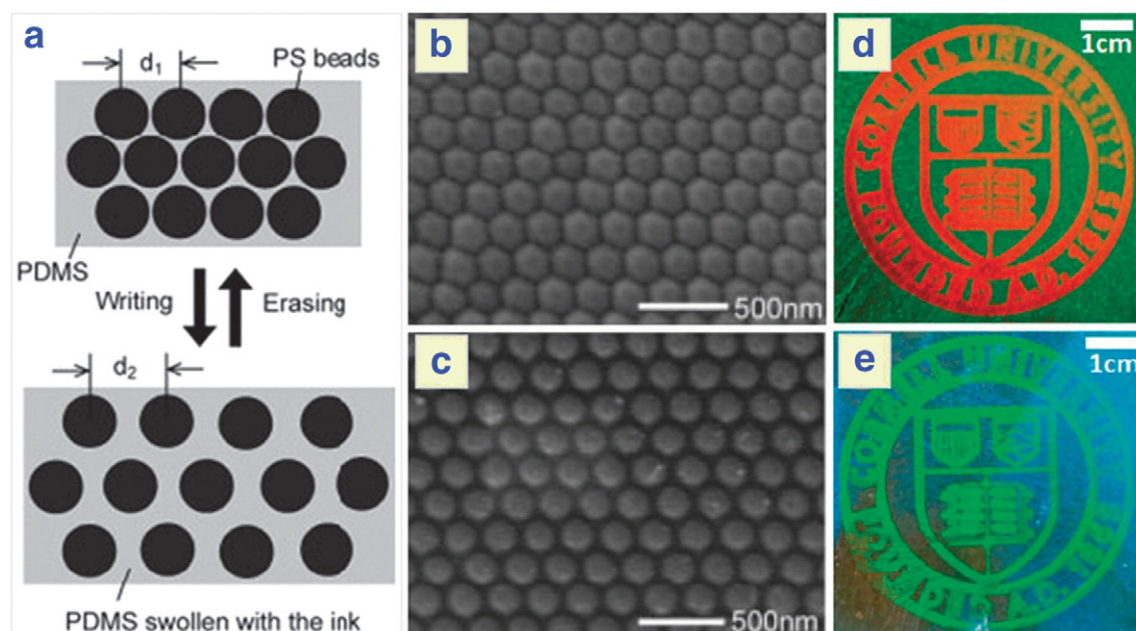


Fig. 26. (a) Schematic of the mechanism of the color's reversibly change: the lattice spacing is increased by swelling the PDMS matrix with the ink. The PDMS matrix shrinks back to its original state once the ink has completely evaporated; (b) SEM image of the (111) plane of a photonic paper-a cubic close-packed lattice of 202 nm PS beads whose void spaces have been completely filled with the PDMS elastomer; (c) SEM image of the same colloidal crystal after it had been swollen with a vinyl-terminated silicone fluid; (d) Demonstration of high resolution multicolor images printed on green substrates; (e) Demonstration of high resolution multicolor images printed on blue substrates. Adapted from reference [109,110] with permission from Wiley and ACS respectively.

matt black ones which also populate the wings. Scanning electron micrographs of the blue scales show that their surfaces comprise a regular two-dimensional array of concavities. By contrast, the matt black scales have fine, sponge-like structure, between the ridges and the cross ribs in the scales. Using both types of scale as bio-templates, they obtained ZnO replicas of the microstructures of the original scales. Both spectra showed a similar sharp near-bandedge emission, but had different green emission, which is associated with the different microstructures of the ZnO replicas [113].

4.3.1. Calcination

Calcination is an elevated-temperature treatment to burn off or decompose the organic materials, as well as to crystallize and densify the ceramic products; but it is not suitable for nano-sized nanocrystalline products and nanostructures because the elevated-temperatures tend to cause heavy aggregation of nanoparticles, coarsen the crystals and cause collapse of nanostructures. Calcination also provides the energy for chemical reactions between the precursor and the underlying template, thus converting as well as consuming the template. During calcination, gaseous products may release, and promote the formation of porous products. Shrinkage generally occurs after calcinations, but at different degrees depending on the template and previous treatments.

4.3.2. Selective dissolution

Selective dissolution is another method to remove templates, which employs corrosive chemicals to dissolve the templates without damaging the products. For example, the silica inverse structure replica of butterfly wing scales was obtained through a sol-gel process and selective dissolution [114,115]. The butterfly wing slices were removed by acid-etching, the whole assembly in a mixture of concentrated nitric acid and perchloric acid while heating at 130 °C for 10–15 min. The slides became separated and transparent when the etching was over. The etched silica inverse structure was yielded at last [116,117]. Fig. 27 shows the different magnification images and a transmission electron microscopy (TEM) image obtained from the SiO₂ inverse structure replica sample.

One drawback of this method is the use of corrosive chemicals, such as the concentrated nitric acid, perchloric acid and ether, which can cause pollution and harmful to health. In order to avoid injury, the products can be isolated by differential dissolution using a solvent when products and the byproducts present different solubility in a solvent. This process is not necessarily corrosive. The selective dissolution could be carried out at mild temperatures, avoiding aggregation of nanoparticles or collapse of nanostructures generally caused by heat treatment. In this sense, selective dissolution for removing templates presents advantages that direct the mineralization of nanomaterials and delicate nanostructures.

4.3.3. Sonication

Sonication is capable of disrupting biologic materials with high-frequency sound waves. Sonication is also energy-conserving compared with calcination that requires elevated temperatures. Moreover, coalescence of nanomaterials and collapse of nanostructures can be avoided due to low-temperature nature of the sonication process. However, its energy is still not enough to destroy and remove hard templates like butterfly wings, and sea urchin plates, which had better be removed by other methods like calcinations and dissolution.

5. Applications

5.1. Self-cleaning super-amphiphobic

Till now, many new commercial products consisting of durable self-cleaning textile fabrics have been designed. Jiang's group developed a two-step procedure to obtain self-cleaning super-amphiphobic (superhydrophobic and superoleophobic) cashmere textiles by low temperature plasma treatment (Fig. 28) [118]. Nanoscale roughness can be introduced on the texture surface after the plasma treatment. The further modification of fluorocarbons will largely decrease the surface energy of the textiles and thus makes the textiles water/oil-repellent. Moreover, the treatments will not change the original properties of

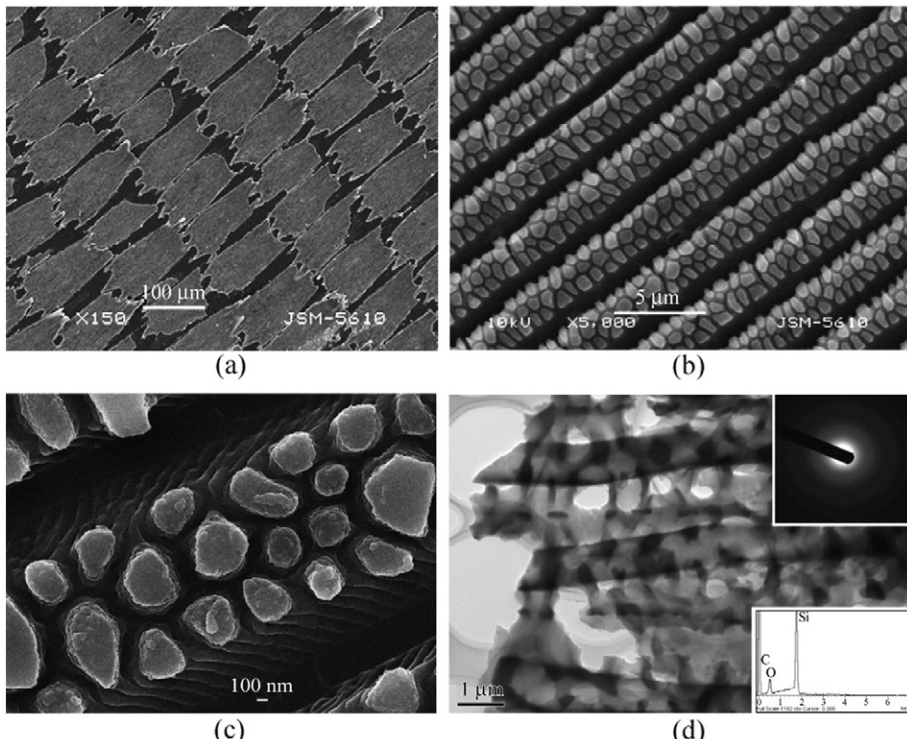


Fig. 27. SEM images of the SiO₂ inverse structure replica. (a) Overview of the surface of the wing scale replica; (b) Medium magnification image of the replica; (c) High-magnification image of the replica; (d) TEM image of the SiO₂ replica of butterfly wing scales. Inset on the right top corner: SAED pattern of the SiO₂ replica. Inset on the right bottom corner: EDX spectrum of the sample. Reproduced from reference [116] with permission from Springer.

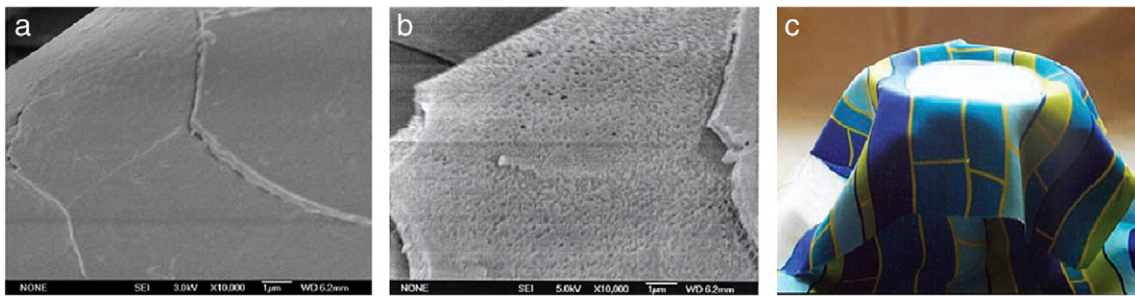


Fig. 28. (a) The SEM image of the untreated cashmere textile; (b) Micro/nano structure on cashmere after plasma treatment; (c) The product of super-amphiphobic textiles. Reproduced from reference [118] with the permission from Wiley.

the textiles, such as color, permeability, soft and flexibility. The oxidation and corrosion of metals in the humid atmosphere limit their application and bring huge waste and environmental contamination. Casting hydrophobic or superhydrophobic coatings on metal surfaces is a probable solution to these problems as the result of the intrinsic water-proof property of the coatings [118]. Superhydrophobic coatings also have applications in eyeglasses, architectures, optical windows for electronic devices, and windows in automobiles [119]. Superhydrophobic coatings have also shown the ability to minimize fluid drag for objects in water [120–123]. Superhydrophobic surfaces are usually superoleophilic, because the low-surface-energy chemicals on superhydrophobic surfaces usually have similar surface energies with the oil drops (hydrocarbon materials). The surface roughness will enhance the oleophilicity, leading to superoleophilicity. One intrinsic application for surfaces integrated with both superhydrophobicity and superoleophilicity is to be used in oil–water separation. Feng et al. firstly reported such application [124].

5.2. Biomimetic adhesion

Recently, a great number of researchers have focused on the sticking ability of geckos. They adhere to surfaces using patches of microscopic hairs that provide a mechanism for dry adhesion through Vander Waals forces. Geckos have the ability to attach to almost any surface, whether wet or dry, smooth or rough. Stickybot [125,126] is a bio-inspired robot that climbs smooth vertical surfaces such as glass, plastic, and ceramic tile. A prototype of "gecko tape" was produced by mimicking arrays of flexible plastic pillars with a geometry optimized for collective adhesion. Polyimide hairs were fabricated using electron-beam lithography and dry etching in oxygen plasma [127]. A Spider-Man toy (15 cm in height and 40 g in weight), used as a demo, was supported by its hand covered by microfabricated gecko tape. A contact area of 0.5 cm^2 was available and the load carrying capacity was noted to be 100 g (Fig. 29).

To seek practical applications of the dry adhesive reported here, Jeong et al. developed a clean transport system by exploiting directional adhesion characteristic. In the liquid crystal display (LCD) industry, a very thin glass substrate (<1 mm thickness) should be accurately transported without surface contamination in vacuum during the process of LCD panel assembly. In particular, suction or mechanical holding is difficult to implement in a vacuum. Currently, an electrostatic chuck (ESC) is used, which is too costly and might lead to surface contamination or damage because of the high electric field applied to the substrate. In this regard, a gecko-inspired dry adhesive has the potential to replace the current ESC holding system because it enables directional adhesion without fouling by sticky materials after many cycles of attachment and detachment. To demonstrate the transport of an LCD glass panel, a simple experimental setup was devised as shown in Fig. 30a and b. The LCD glass used in this experiment was 0.9 mm in thickness and $47.5 \times 37.5 \text{ cm}^2$ in size. Before attachment to the glass panel, a dry adhesive ($3 \times 3 \text{ cm}^2$) was attached to the moving unit, which then approached the glass, forming a conformal contact with the aid of a thin PDMS block and a sponge-like cushion that had been sealed onto the back side of the dry adhesive and the glass panel, respectively. After forming firm attachment of the dry-adhesive with nanohairs drooping downward, the moving unit started to move upward, lifting the glass panel by the shear adhesion of the dry adhesive. After arriving at a target location, the moving unit started to move downward, releasing the panel from the adhesive with the aid of a support box that had been placed on a releasing position. The support box acted as a separator from the adhesive when pulling the dry adhesive along the opposite direction [128].

5.3. Biomimetic non-adhesive

Many countries devote large resources to invent new kinds of non-stick pots because the non-stick pots made of Teflon coat has potential harm to human body. It was demonstrated that cuticles of some animals

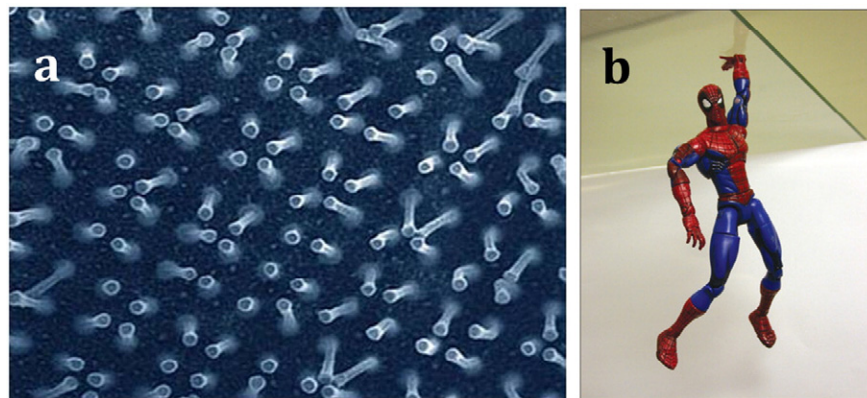


Fig. 29. (a) Polyimide hairs fabricated to form the gecko tape and (b) a spider-man toy clinging to a horizontal glass plate by microfabricated gecko tape on the hand. Adapted from reference [127] with permission from Nature Publishing Group.

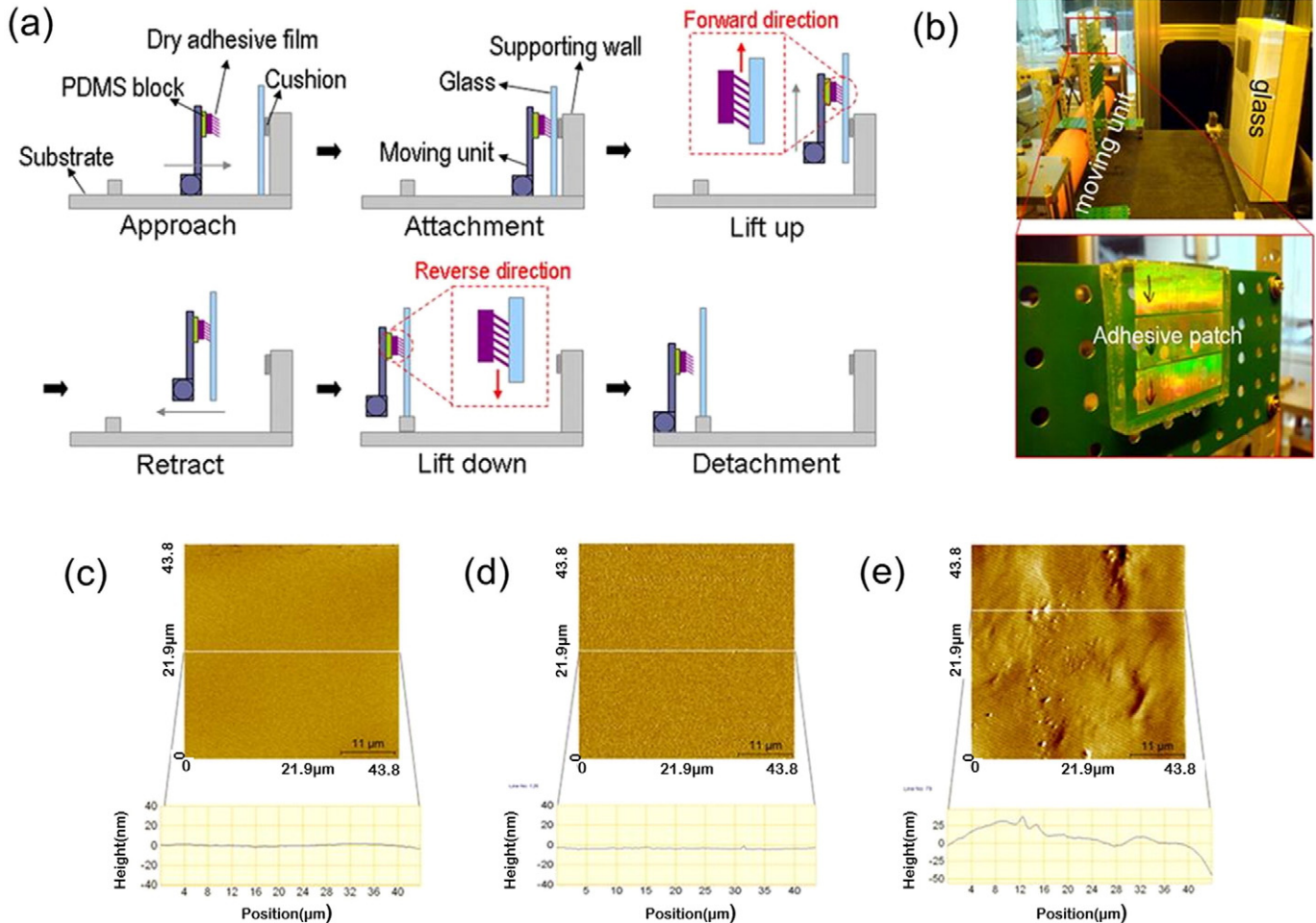


Fig. 30. Demonstration of the clean transportation system with a dry adhesive patch. (a) A schematic illustration of the LCD transport process with a gecko inspired dry adhesive. When the adhesive patch is pulled along the forward direction, the glass panel can be firmly lifted, whereas it can be easily detached by pulling the patch along the opposite direction; (b) A photograph of the LCD glass transport system (Upper) and a magnified photograph showing the dry-adhesive patch integrated with the system (Lower); (c) and (d) Two dimensional AFM micrographs and corresponding cross-sectional profiles of the glass surface before (c) and after (d) attachment of the dry adhesive; (e) A two-dimensional AFM micrograph and the corresponding surface profile of the glass surface after attachment of a pressure-sensitive tape. The surface was fouled with sticky molecules transferred from the tape. Reproduced from reference [128].

such as dung beetle and ground beetle, display the varied textured morphologies, such as the convex domes (Fig. 31a), dimpled or scaly form morphologies [129]. The morphologies are the results of the optimization for survival of the animals. It was shown that the textured morphologies possess high anti-adhesion properties. Ren's group designed biomimetic surfaces non-adhesive cooker with convex domes, as shown in Fig. 31b. The production of bionic non-adhesive cooker was punched the convex surface on the inner surface by means of

mold punch. The practicability test result showed the anti-adhesion ability of the bionic non-adhesive cooker was equal to that of Teflon cooker.

5.4. Engineering drag-reduction

The studies of shark skin have led to drag-reducing coatings [52]. The ribbed texture of the scales of a shark (Fig. 32), just visible under

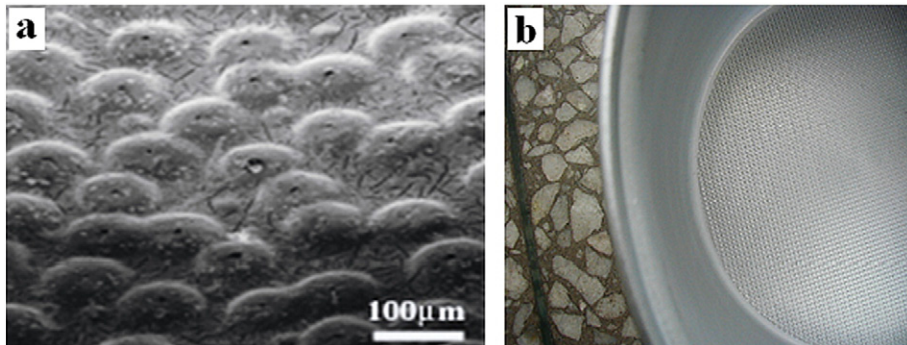


Fig. 31. (a) Dung beetle convex domes morphologies; (b) Bionic non-adhesive cooker. Adapted from reference [129] with permission from Springer.

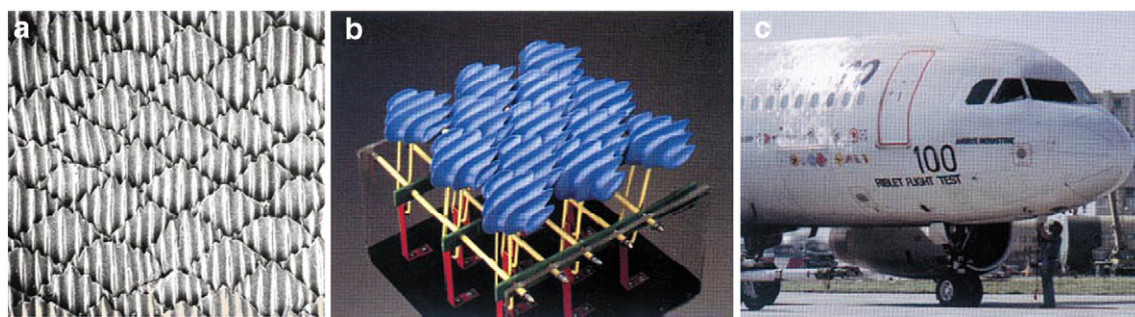


Fig. 32. Corrugated coating for drag reduction. (a) The riblets on shark skin; (b) Inspiration modeling studies of the drag reduction; (c) Trials on an aircraft coated with a plastic film with this same microscopic texture. Adapted from reference [51] with permission from Nature Publishing Group.

a magnifying glass, seems to provide aerodynamic efficiency relative to a smooth surface because of the way that the corrugations affect the viscous boundary layer of the water. A transparent plastic film with this same microscopic texture, ribs parallel to the direction of flow, helps to reduce aircraft drag by up to 8% - representing a fuel saving of about 1.5% [51].

Inspired by natural design, scientists are adding technological improvements to swimming suits by designing antimicrobial fabrics without the chemical treatments, especially in Olympic swimming competitions. Now such important sport events are heading towards technological support since swimmers are using swimming suit designed on the hydrodynamics principles of a shark's skin. These tightly fitting suits, covering rather a large area of the body are made up of fabrics which are designed to mimic the properties of a shark's skin by superimposing vertical resin stripes. This phenomenon is known as the Riblet effect (Fig. 33). Swimsuits made with the new fibers and weaving techniques mimicking shark scales microfeatures, are produced to cling tightly to the swimmer's body. It may give the wearer a 6-m equivalent head start in swimming competition by dampening turbulence in the immediate layer of water, next to the skin [130].

Animal functional surfaces have broad application space. Structure color from animal body surface [54,131–138] can also be used for video stealth research. Aircraft engines and helicopter rotor-blades erosion are constantly abraded by atmospheric dust, and a way of slowing

down this abrasion would be welcome. A little surface irregularity might help to prolong the active lives of planes and helicopters, as well as those of scorpions [25]. The surface of the compound eye is covered by highly packed protuberances, which potentially increases visual efficiency through increased photon capture for a given stimulus. The compound eye replica with antireflective structure exhibits great potential in the applications of optical coating, sensing or lens arrays [139–141]. With the adhesion theory, bionic drill with anti-adhesion and anti-resistance characters will have good prospects [24,129].

6. Summary

Learning from natural creatures could simplify the development of advanced artificial functional surfaces. Over the past several decades, considerable efforts have been devoted to biomimetic fabrication of multiscale structures for multifunction integration. Mimicking natural masterpieces, the obtained artificial materials would exhibit both multiscale structures and superior properties similar to or even better than that of biomaterials. This makes the biomimetic fabrication a promising approach for the rational design and manufacture of various high-performance man-made devices [142].

Properties of animals' functional surfaces result from a complex interplay between surface morphology and physical and chemical properties. Hierarchical structures with dimensions of features ranging from

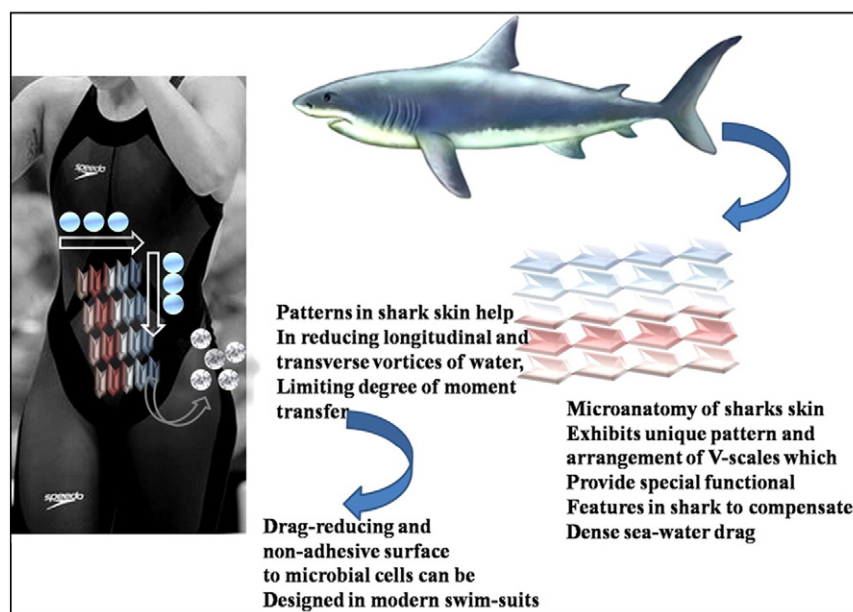


Fig. 33. Shark skin feature inspired low hydrodynamic surface drag: high efficiency swimsuits design with antibacterial effect. Nature's unique design at microscale provides enormous reduction in surface drag of water close to the body (Riblet effect). Arrows show anti-microbial features mimicking shark skin micro-topography. Reproduced from reference [130] with permission from Elsevier.

the macroscale to the nanoscale are extremely common in nature to provide properties of interest [38]. Animals have learned how to achieve most efficient multi-functional surfaces. The optimized biological solution should give us inspiration and design principles for the construction of multi-functional artificial surfaces. In the last few decades, inspired by the typical animals' functional surfaces, a great number of multi-functional surfaces have been fabricated. This article has focused on the typical animals' surfaces with drag reduction, noise reduction, anti-adhesion, anti-wear, anti-erosion, anti-stealthy, anti-fog, low reflection of light, and others. The development of animal functional surfaces is important for basic research as well as various applications, including super-amphiphobic textiles, self-cleaning nano-tie, stickybot and applications requiring anti-fouling and a reduction in fluid flow. These surfaces can also be used in energy conversion and conservation.

In the near future, the following research directions should be a growing and vigorous field. (i) To extend the new function of animals' functional surface; (ii) Clarification of structure-multipurpose relationship; (iii) The construction of animals' functional surfaces. Although the biomimetic and bio-inspired research is in its infancy, it is a rapidly growing and enormously promising field, which will become the focus of international competition in the near future. This article provides a useful guide for the development of biomimetic artificial surfaces. Now, interdisciplinary cooperation is necessary for researchers in the area of science and engineering to further investigate the animals' functional surfaces and discover the new function. The increasing collaboration work would also be useful for the improved understanding of structure-function relationship, extraction of useful engineering principles, and adaptation of models for practical applications.

Acknowledgements

This work is supported by the National Natural Science Foundation of China (Nos. 51325501, 51505183, 51175220 51290292 and 51205161), China Postdoctoral Science Foundation Funded Project (No. 2015M571360) and The 13th Five-Year Scientific Research Project of Education Department of Jilin Province (Nos. 2015474, 2015492).

References

- [1] Bhushan B. Biomimetics: lessons from nature—an overview. *Phil Trans R Soc A* 2009;367:1445–86.
- [2] Sanchez C, Arribart H, Guille MMG. Biomimetic and bioinspiration as tools for the design of innovative materials and systems. *Nat Mater* 2005;4:277–88.
- [3] Han ZW, Wu LY, Qiu ZM, Ren LQ. Microstructure and structural color in wing scales of butterfly *Thaumantis diocles*. *Chin Sci Bull* 2009;54:535–40.
- [4] Chen K, Liu QP, Liao GH, Yang Y, Ren LQ, Yang HX, et al. The sound suppression characteristics of wing feather of owl (*Bubo bubo*). *J Bionic Eng* 2012;9:192–9.
- [5] Gao XF, Jiang L. Water-repellent legs of water striders. *Nature* 2004;432:36.
- [6] Kemp DJ. Female mating biases for bright ultraviolet iridescence in the butterfly *Eurema hecabe* (Pieridae). *Behav Ecol* 2008;19:1–8.
- [7] Kemp DJ. Female butterflies prefer males bearing bright iridescent ornamentation. *Proc R Soc B* 2007;274:1043–7.
- [8] Sweeney A, Jiggins C, Johnsen S. Insect communication: Polarized light as a butterfly mating signal. *Nature* 2003;423:31–2.
- [9] Papke RS, Kemp DJ, Rutowski RL. Multimodal signalling: structural ultraviolet reflectance predicts male mating success better than pheromones in the butterfly *Colias eurytheme* L. (Pieridae) (vol 73, pg 47, 2007). *Anim Behav* 2007;73:1083.
- [10] Kemp DJ. Ultraviolet ornamentation and male mating success in a high-density assemblage of the butterfly *Colias eurytheme*. *J Insect Behav* 2006;19:669–84.
- [11] Liu KS, Yao X, Jiang L. Recent developments in bio-inspired special wettability. *Chem Soc Rev* 2010;39:3240–55.
- [12] Huebsch N, Mooney DJ. Inspiration and application in the evolution of biomaterials. *Nature* 2009;462:426–32.
- [13] Lee LP, Szema R. Inspirations from biological, optics for advanced photonic systems. *Science* 2005;310:1148–50.
- [14] Liu MJ, Zheng YM, Zhai J, Jiang L. Bioinspired super-antiwetting interfaces with special liquid-solid adhesion. *Acc Chem Res* 2010;43:368–77.
- [15] Xia F, Jiang L. Bio-inspired, smart, multiscale interfacial materials. *Adv Mater* 2008;20:2842–58.
- [16] Li YF, Zhang JH, Yang B. Antireflective surfaces based on biomimetic nanopillared arrays. *Nano Today* 2010;5:117–27.
- [17] Liu KS, Jiang L. Metallic surfaces with special wettability. *Nanoscale* 2011;3:825–38.
- [18] Nosonovsky M, Bhushan B. Green tribology: principles, research areas and challenges introduction. *Phil Trans R Soc A* 2010;368:4677–94.
- [19] Tong J, Zhang ZH, Ma YH, Chen DH, Jia BY, Menon C. Abrasive wear of embossed surfaces with convex domes. *Wear* 2012;274:196–202.
- [20] Aizenberg J, Fratzl P. Biological and biomimetic materials. *Adv Mater* 2009;21:387–8.
- [21] Tian XM, Han ZW, Li XJ, Pu ZG, Ren LQ. Biological coupling anti-wear properties of three typical molluscan shells-*Scapharca subcrenata*, *Rapana venosa* and *Acanthochiton rubrolineatus*. *SCIENCE CHINA Technol Sci* 2010;53:2905–13.
- [22] Tong J, Wang H, Ma Y, Ren L. Two-body abrasive wear of the outside shell surfaces of mollusc *Lamprotula fibrosa heude*, *Rapana venosa valenciennes* and *dosinia anus philippi*. *Tribol Lett* 2005;19:331–8.
- [23] Tong J, Mohammad MA, Zhang JB, Ma YH, Rong BJ, Chen DH, et al. DEM numerical simulation of abrasive wear characteristics of a bioinspired ridged surface. *J Bionic Eng* 2010;7:175–81.
- [24] Ren LQ, Tong J, Li JQ, Chen BC. Soil adhesion and biomimetics of soil-engaging components: a review. *J Agric Eng Res* 2001;79:239–63.
- [25] Han ZW, Zhang JQ, Ge C, Wen L, Ren LQ. Erosion resistance of bionic functional surfaces inspired from desert scorpions. *Langmuir* 2012;28:2914–21.
- [26] Han ZW, Zhang JQ, Ge C, Lu Y, Jiang JL, Liu QP, et al. Anti-erosion function in animals and its biomimetic application. *J Bionic Eng* 2010;7:S50–8.
- [27] Han ZW, Zhang JQ, Ge C, Jiang JL, Ren LQ. Gas-solid erosion on bionic configuration surface. *J Wuhan Univ Technol* 2011;26:306–11.
- [28] Yan YY, Gao N, Barthlott W. Mimicking natural superhydrophobic surfaces and grasping the wetting process: A review on recent progress in preparing superhydrophobic surfaces. *Adv Colloid Interface Sci* 2011;169:80–105.
- [29] Feng L, Zhang YA, Xi JM, Zhu Y, Wang N, Xia F, et al. Petal effect: A superhydrophobic state with high adhesive force. *Langmuir* 2008;24:4114–9.
- [30] Koch K, Bhushan B, Barthlott W. Diversity of structure, morphology and wetting of plant surfaces. *Soft Matter* 2008;4:1943–63.
- [31] Fang Y, Sun G, Cong Q, Chen GH, Ren LQ. Effects of methanol on wettability of the non-smooth surface on butterfly wing. *J Bionic Eng* 2008;5:127–33.
- [32] Byun D, Hong J, Saputra, Ko JH, Lee YJ, Park HC, et al. Wetting characteristics of insect wing surfaces. *J Bionic Eng* 2009;6:63–70.
- [33] Barnes WJP. Biomimetic solutions to sticky problems. *Science* 2007;318:203–4.
- [34] Tuteja A, Choi W, Ma ML, Mabry JM, Mazzella SA, Rutledge GC, et al. Designing superoleophobic surfaces. *Science* 2007;318:1618–22.
- [35] Sung YH, Kim YD, Choi HJ, Shin R, Kang S, Lee H. Fabrication of superhydrophobic surfaces with nano-in-micro structures using UV-nanoimprint lithography and thermal shrinkage films. *Appl Surf Sci* 2015;349:169–73.
- [36] Fang Y, Sun G, Wang TQ, Cong Q, Ren LQ. Hydrophobicity mechanism of non-smooth pattern on surface of butterfly wing. *Chin Sci Bull* 2007;52:711–6.
- [37] Sun G, Fang Y, Cong Q, Ren LQ. Anisotropism of the non-smooth surface of butterfly wing. *J Bionic Eng* 2009;6:71–6.
- [38] Bhushan B, Jung YC. Natural and biomimetic artificial surfaces for superhydrophobicity, self-cleaning, low adhesion, and drag reduction. *Prog Mater Sci* 2011;56:1–108.
- [39] Gao HJ, Wang X, Yao HM, Gorb S, Arzt E. Mechanics of hierarchical adhesion structures of geckos. *Mech Mater* 2005;37:275–85.
- [40] Bhushan B, Peressadko AG, Kim TW. Adhesion analysis of two-level hierarchical morphology in natural attachment systems for 'smart adhesion'. *J Adhes Sci Technol* 2006;20:1475–91.
- [41] Autumn K. How gecko toes stick - the powerful, fantastic adhesive used by geckos is made of nanoscale hairs that engage tiny forces, inspiring envy among human imitators. *Am Sci* 2006;94:124–32.
- [42] Bhushan B, Sayer RA. Surface characterization and friction of a bio-inspired reversible adhesive tape. *Microsyst Technol* 2007;13:71–8.
- [43] Kim TW, Bhushan B. Adhesion analysis of multi-level hierarchical attachment system contacting with a rough surface. *J Adhes Sci Technol* 2007;21:1–20.
- [44] Kim TW, Bhushan B. Effect of stiffness of multi-level hierarchical attachment system on adhesion enhancement. *Ultramicroscopy* 2007;107:902–12.
- [45] Fratzl P. Biomimetic materials research: what can we really learn from nature's structural materials? *J R Soc Interface* 2007;4:637–42.
- [46] Autumn K, Liang YA, Hsieh ST, Zesch W, Chan WP, Kenny TW, et al. Adhesive force of a single gecko foot-hair. *Nature* 2000;405:681–5.
- [47] Filippov AE, Gorb SN. Spatial model of the gecko foot hair: functional significance of highly specialized non-uniform geometry. *Interface Focus* 2015;5:20140065.
- [48] Bhushan B, Sayer RA. Gecko feet: natural attachment systems for smart adhesion. *Applied Scanning Probe Methods VII*; 2007. p. 41–76.
- [49] Liu MJ, Wang ST, Wei ZX, Song YL, Jiang L. Bioinspired design of a superoleophobic and low adhesive water/solid interface. *Adv Mater* 2009;21:665–9.
- [50] Liu KS, Jiang L. Bio-inspired design of multiscale structures for function integration. *Nano Today* 2011;6:155–75.
- [51] Ball P. Engineering - shark skin and other solutions. *Nature* 1999;400:507–9.
- [52] Bechert DW, Bruse M, Hage W. Experiments with three-dimensional ripples as an idealized model of shark skin. *Exp Fluids* 2000;28:403–12.
- [53] Dean B, Bhushan B. Shark-skin surfaces for fluid-drag reduction in turbulent flow: A review. *Phil Trans R Soc A* 2010;368:4775–806.
- [54] Han ZW, Niu SC, Shang CH, Liu ZN, Ren LQ. Light trapping structures in wing scales of butterfly *Trogonoptera brookiana*. *Nanoscale* 2012;4:2879–83.
- [55] Han ZW, Wu LY, Qiu ZM, Guan HY, Ren LQ. Structural colour in butterfly *Apatura ilia* scales and the microstructure simulation of photonic crystal. *J Bionic Eng* 2008;5:14–9.

- [56] Wu LY, Ren WT, Song YQ, Xin MJ, Niu SC, Han ZW. High light absorption properties and optical structures in butterfly *Heliothis vires* wing scales. RSC Adv 2015;5:46011–6.
- [57] Han ZW, Li B, Mu ZZ, Yang M, Niu SC, Zhang JQ, et al. An ingenious super light trapping surface templated from butterfly wing scales. Nanoscale Res Lett 2015; 10:344.
- [58] Genzer J, Efimenco K. Recent developments in superhydrophobic surfaces and their relevance to marine fouling: A review. Biofouling 2006;22:339–60.
- [59] Gao XF, Yan X, Yao X, Xu L, Zhang K, Zhang JH, et al. The dry-style antifogging properties of mosquito compound eyes and artificial analogues prepared by soft lithography. Adv Mater 2007;19:2213–7.
- [60] Parker AR, Lawrence CR. Water capture by a desert beetle. Nature 2001;414:33–4.
- [61] Zhai L, Berg MC, Cebeci FC, Kim Y, Milwid JM, Rubner MF, et al. Patterned superhydrophobic surfaces: Toward a synthetic mimic of the Namib Desert beetle. Nano Lett 2006;6:1213–7.
- [62] Garrod RP, Harris LG, Schofield WCE, McGettrick J, Ward LJ, Teare DOH, et al. Mimicking a stenocara beetle's back for microcondensation using plasmachemical patterned superhydrophobic-superhydrophilic surfaces. Langmuir 2007;23:689–93.
- [63] Hansen WR, Autumn K. Evidence for self-cleaning in gecko setae. Proc Natl Acad Sci U S A 2005;102:385–9.
- [64] Autumn K. Gecko adhesion: structure, function, and applications. MRS Bull 2007; 32:473–8.
- [65] Hu DL, Chan B, Bush JWM. The hydrodynamics of water strider locomotion. Nature 2003;424:663–6.
- [66] Baumli P, Kaptyag G. Wettability of carbon surfaces by pure molten alkali chlorides and their penetration into a porous graphite substrate. Mater Sci Eng A 2008;495: 192–6.
- [67] Autumn K, Hansen W. Ultrahydrophobicity indicates a non-adhesive default state in gecko setae. J Comp Physiol A 2006;192:1205–12.
- [68] Liu KS, Du JX, Wu JT, Jiang L. Superhydrophobic gecko feet with high adhesive forces towards water and their bio-inspired materials. Nanoscale 2012;4:768–72.
- [69] Feng L, Li SH, Li YS, Li HJ, Zhang LJ, Zhai J, et al. Super-hydrophobic surfaces: from natural to artificial. Adv Mater 2002;14:1857–60.
- [70] Tie L, Guo ZG, Liu WM. Anisotropic wetting properties on various shape of parallel grooved microstructure. J Colloid Interface Sci 2015;453:142–50.
- [71] Wang ST, Liu KS, Yao X, Jiang L. Bioinspired surfaces with superwettability: new insight on theory, design, and applications. Chem Rev 2015;115:8230–93.
- [72] Kwon MH, Shin HS, Chu CN. Fabrication of a super-hydrophobic surface on metal using laser ablation and electrodeposition. Appl Surf Sci 2014;288:222–8.
- [73] Zheng YM, Gao XF, Jiang L. Directional adhesion of superhydrophobic butterfly wings. Soft Matter 2007;3:178–82.
- [74] Nakajima A, Hashimoto K, Watanabe T. Recent studies on super-hydrophobic films. Monatsh Chem 2001;132:31–41.
- [75] Jarn M, Granqvist B, Lindfors J, Kallio T, Rosenholm JB. A critical evaluation of the binary and ternary solid-oil–water and solid-water–oil interaction. Adv Colloid Interface Sci 2006;123:137–49.
- [76] Gao J, Yao X, Zhao Y, Jiang L. Lyophilic nonwettable surface based on an oil/water/air/solid four-phase system. Small 2013;9:2515–9.
- [77] Autumn K, Dittmore A, Santos D, Spenko M, Cutkosky M. Frictional adhesion: A new angle on gecko attachment. J Exp Biol 2006;209:3569–79.
- [78] Hui CY, Glassmaker NJ, Tang T, Jagota A. Design of biomimetic fibrillar interfaces: 2. mechanics of enhanced adhesion. J R Soc Interface 2004;1:35–48.
- [79] Gay C. Stickiness – some fundamentals of adhesion. Integr Comp Biol 2002;42:1123–6.
- [80] Ingram AL, Parker AR. A review of the diversity and evolution of photonic structures in butterflies, incorporating the work of John Huxley (the Natural History Museum, London from 1961 to 1990). Philos Trans R Soc B 2008;363:2465–80.
- [81] Luchini P, Manzo F, Pozzi A. Resistance of a grooved surface to parallel flow and cross-flow. Int J Fluid Mech Res 1991;228:87–109.
- [82] Bechert DW, Bruse M, Hage W, Hoeven JGTV, Hoppe G. Experiments on drag-reducing surfaces and their optimization with an adjustable geometry. Int J Fluid Mech Res 1997;338:59–87.
- [83] Fan T-X, Chow S-K, Zhang D. Biomimetic mineralization: from biology to materials. Prog Mater Sci 2009;54:542–659.
- [84] Zhang T, Li MZ, Su B, Ye CQ, Li K, Shen WZ, et al. Bio-inspired anisotropic micro/nano-surface from a natural stamp: Grasshopper wings. Soft Matter 2011;7: 7973–5.
- [85] Caruso RA, Antonietti M. Sol-gel nanocoating: an approach to the preparation of structured materials. Chem Mater 2001;13:3272–82.
- [86] Teo CJ, Khoo BC. Analysis of Stokes flow in microchannels with superhydrophobic surfaces containing a periodic array of micro-grooves. Microfluid Nanofluid 2009; 7:353–82.
- [87] Kim Y, Jung E, Yim M. Fabrication of discrete materials by interface-selective sol-gel polymerization. Chem Lett 2002:992–3.
- [88] Kim Y. Small structures fabricated using ash-forming biological materials as templates. Biomacromolecules 2003;4:908–13.
- [89] Zang XN, Ge YY, Gu JJ, Zhu SM, Su HL, Feng CL, et al. Tunable optical photonic devices made from moth wing scales: A way to enlarge natural functional structures pool. J Mater Chem 2011;21:13913–9.
- [90] Zhang ZL, Yu K, Lou L, Yin HH, Li B, Zhu ZQ. Morphology-controlled synthesis of ZnO replicas with photonic structures from butterfly (*Papilio paris*) wing scales for tunable optical properties. Nanoscale 2012;4:2606–12.
- [91] Cook G, Timms PL, Spickermann CG. Exact replication of biological structures by chemical vapor deposition of silica. Angew Chem Int Ed 2003;42:557–9.
- [92] Zhang W, Zhang D, Fan T, Ding J, Gu J, Guo Q, et al. Biomimetic zinc oxide replica with structural color using butterfly (*Ideopsis similis*) wings as templates. Bioinspir Biomim 2006;1:89–95.
- [93] Silver J, Withnall R, Ireland TG, Fern GR. Novel nano-structured phosphor materials cast from natural *Morpho* butterfly scales. J Mod Opt 2005;52:999–1007.
- [94] Leem JW, Chung KS, Yu JS. Antireflective properties of disordered Si SWs with hydrophobic surface by thermally dewetted Pt nanomask patterns for Si-based solar cells. Curr Appl Phys 2012;12:291–8.
- [95] Li YF, Zhang JH, Zhu SJ, Dong HP, Jia F, Wang ZH, et al. Biomimetic surfaces for high-performance optics. Adv Mater 2009;21:4731–4.
- [96] Min WL, Jiang B, Jiang P. Bioinspired self-cleaning antireflection coatings. Adv Mater 2008;20:3914–8.
- [97] Li YF, Li F, Zhang JH, Wang CL, Zhu SJ, Yu HJ, et al. Improved light extraction efficiency of white organic light-emitting devices by biomimetic antireflective surfaces. Appl Phys Lett 2010;96:153305.
- [98] Kanamori Y, Ishimori M, Hane K. High efficient light-emitting diodes with antireflection subwavelength gratings. IEEE Photon Technol Lett 2002;14:1064–6.
- [99] Zhu SM, Zhang D, Li ZQ, Furukawa H, Chen ZX. Precision replication of hierarchical biological structures by metal oxides using a sonochemical method. Langmuir 2008;24:6292–9.
- [100] Watanabe K, Hoshino T, Kanda K, Haruyama Y, Matsui S. Brilliant blue observation from a *Morpho*-butterfly-scale quasi-structure. Jpn J Appl Phys 2005;2(44):148–50.
- [101] Elam JW, Routkевич D, Mardilovich PP, George SM. Conformal coating on ultrahigh-aspect-ratio nanopores of anodic alumina by atomic layer deposition. Chem Mater 2003;15:3507–17.
- [102] Huang J, Wang X, Wang ZL. Controlled replication of butterfly wings for achieving tunable photonic properties. Nano Lett 2006;6:2325–31.
- [103] Kolle M, Salgad-Cunha PM, Scherer MRJ, Huang FM, Vukusic P, Mahajan S, et al. Mimicking the colourful wing scale structure of the *Papilio blumei* butterfly. Nat Nanotechnol 2010;5:511–5.
- [104] Ritala M, Kulki K, Rahtu A, Raisanen PI, Leskela M, Sajavaara T, et al. Atomic layer deposition of oxide thin films with metal alkoxides as oxygen sources. Science 2000; 288:319–21.
- [105] Linn NC, Sun C-H, Jiang P, Jiang B. Self-assembled biomimetic antireflection coatings. Appl Phys Lett 2007;91:101108.
- [106] Zhang D, Zhang W, Gu JJ, Fan TX, Liu QL, Su HL, et al. Inspiration from butterfly and moth wing scales: characterization, modeling, and fabrication. Prog Mater Sci 2015;68:67–96.
- [107] Chung K, Yu S, Heo CJ, Shim JW, Yang SM, Han MG, et al. Flexible, angle-independent, structural color reflectors inspired by *Morpho* butterfly wings. Adv Mater 2012;24:2375–9.
- [108] Ho YH, Liu CC, Liu SW, Liang H, Chu CW, Wei PK. Efficiency enhancement of flexible organic light-emitting devices by using antireflection nanopillars. Opt Express 2011;19:A295–302.
- [109] Kang PG, Ogunbo SO, Erickson D. High resolution reversible color images on photonic crystal substrates. Langmuir 2011;27:9676–80.
- [110] Fudouzi H, Xia YN. Photonic papers and inks: color writing with colorless materials. Adv Mater 2003;15:892–6.
- [111] Chrisey DB. Materials processing—The power of direct writing. Science 2000;289: 879–81.
- [112] Turner MD, Schroder-Turk GE, Gu M. Fabrication and characterization of three-dimensional biomimetic chiral composites. Opt Express 2011;19:10001–8.
- [113] Zhang W, Zhang D, Fan TX, Ding J, Gu JJ, Guo Q, et al. Biosynthesis of cathodoluminescent zinc oxide replicas using butterfly (*Papilio paris*) wing scales as templates. Mater Sci Eng C Biomim Supramol Syst 2009;29:92–6.
- [114] Han ZW, Niu SC, Yang M, Zhang JQ, Yin W, Ren LQ. An ingenious replica templated from the light trapping structure in butterfly wing scales. Nanoscale 2013;5: 8500–6.
- [115] Han ZW, Niu SC, Li W, Ren LQ. Preparation of bionic nanostructures from butterfly wings and their low reflectivity of ultraviolet. Appl Phys Lett 2013;102:233702.
- [116] Xu Z, Yu K, Li B, Huang R, Wu P, Mao HB, et al. Optical properties of SiO₂ and ZnO nanostructured replicas of butterfly wing scales. Nano Res 2011;4:737–45.
- [117] Han ZW, Mu ZZ, Li B, Niu SC, Zhang JQ, Ren LQ. A high-transmission, multiple anti-reflective surface inspired from bilayer 3D ultrafine hierarchical structures in butterfly wing scales. Small 2016;12:713–20.
- [118] Yao X, Song YL, Jiang L. Applications of bio-inspired special wettability surfaces. Adv Mater 2011;23:719–34.
- [119] Zhang X, Shi F, Niu J, Jiang YG, Wang ZQ. Superhydrophobic surfaces: from structural control to functional application. J Mater Chem 2008;18:621–33.
- [120] Ou J, Perot B, Rothstein JP. Laminar drag reduction in microchannels using ultrahydrophobic surfaces. Phys Fluids 2004;16:4635–43.
- [121] Ou J, Rothstein JP. Direct velocity measurements of the flow past drag-reducing ultrahydrophobic surfaces. Phys Fluids 2005;17:103606.
- [122] Truesdell R, Mammoli A, Vorobieff P, van Swol F, Brinker CJ. Drag reduction on a patterned superhydrophobic surface. Phys Rev Lett 2006;97:044504.
- [123] Rastegari A, Akhavan R. On the mechanism of turbulent drag reduction with superhydrophobic surfaces. J Fluid Mech 2015;773:R4.
- [124] Feng L, Zhang ZY, Mai ZH, Ma YM, Liu BQ, Jiang L, et al. A super-hydrophobic and super-oleophobic coating mesh film for the separation of oil and water. Angew Chem Int Ed 2004;43:2012–4.
- [125] Asbeck A, Dastoor S, Parness A, Fullerton L, Esparza N, Soto D, et al. Climbing rough vertical surfaces with hierarchical directional adhesion. ICRA: 2009 IEEE International Conference on Robotics and Automation, 1–7; 2009. p. 4328–33.
- [126] Soto D, Hill G, Parness A, Esparza N, Cutkosky M, Kenny T. Effect of fibril shape on adhesive properties. Appl Phys Lett 2010;97:053701.
- [127] Geim AK, Dubonos SV, Grigorieva IV, Novoselov KS, Zhukov AA, Shapoval SY. Microfabricated adhesive mimicking gecko foot-hair. Nat Mater 2003;2:461–3.
- [128] Jeong HE, Lee JK, Kim HN, Moon SH, Suh KY. A nontransferring dry adhesive with hierarchical polymer nanohairs. Proc Natl Acad Sci U S A 2009;106:5639–44.

- [129] Ren LQ. Progress in the bionic study on anti-adhesion and resistance reduction of terrain machines. *Sci China Ser E* 2009;52:273–84.
- [130] Singh AV, Rahman A, Kumar NVGS, Aditi AS, Galluzzi M, Bovio S, et al. Bio-inspired approaches to design smart fabrics. *Mater Des* 2012;36:829–39.
- [131] McPhedran RC, Nicorovici NA, McKenzie DR, Rouse GW, Botten LC, V W, et al. Structural colours through photonic crystals. *Physica B* 2003;338:182–5.
- [132] Parker AR. A vision for natural photonics. *Phil Trans R Soc A* 2004;362:2709–20.
- [133] Brink DJ, van der Berg NG. Structural colours from the feathers of the bird *Bostrychia hagedash*. *J Phys D Appl Phys* 2004;37:813–8.
- [134] Wong TH, Gupta MC, Robins B, Levendusky TL. Color generation in butterfly wings and fabrication of such structures. *Opt Lett* 2003;28:2342–4.
- [135] Plattner L. Optical properties of the scales of *Morpho rhetenor* butterflies: theoretical and experimental investigation of the back-scattering of light in the visible spectrum. *J R Soc Interface* 2004;1:49–59.
- [136] Parker AR, Hegedus Z. Diffractive optics in spiders. *J Opt A Pure Appl Opt* 2003;5: S111–6.
- [137] Niu SC, Li B, Mu ZZ, Yang M, Zhang JQ, Han ZW, et al. Excellent structure-based multifunction of *Morpho* butterfly wings: A review. *J Bionic Eng* 2015;12:170–89.
- [138] Han ZW, Niu SC, Yang M, Mu ZZ, Li B, Zhang JQ, et al. Unparalleled sensitivity of photonic structures in butterfly wings. *RSC Adv* 2014;4:45214–9.
- [139] Huang JY, Wang XD, Wang ZL. Bio-inspired fabrication of antireflection nanostructures by replicating fly eyes. *Nanotechnology* 2008;19.
- [140] Stavenga DG. Reflections on colourful ommatidia of butterfly eyes. *J Exp Biol* 2002; 205:1077–85.
- [141] Stavenga DG. Colour in the eyes of insects. *J Comp Physiol A* 2002;188:337–48.
- [142] Zhang Y, Chen Q-D, Jin Z, Kim E, Sun H. Biomimetic graphene films and their properties. *Nanoscale* 2012;4:4858–69.